

DOI: <https://doi.org/10.24297/jap.v22i.9633>**Prototyping a Disruptive Self-Sustaining Power Plant enabled to overcome Perpetual Motion Machines**

Ramon Ferreiro Garcia (independent author)

Former Prof. Emeritus at the University of A Coruna, Spain

<https://www.udc.es>, ramon.ferreiro@udc.es**Abstract;**

This research discusses a strategic methodology for implementing a disruptive Self-Sustaining Power Plant (SSPP) characterized by the cascading coupling of a group of Power Units (PUs). In this configuration, the heat released from each PU due to the cooling of the thermal working fluid (TWF) is efficiently recovered and reused as supply heat for the first PU in the cascade.

Two case studies on the SSPP have been conducted using air and helium as TWFs. The first deals with PUs coupled in cascade operating with closed processes-based V_{sp} thermal cycles, while the second involves PUs coupled in cascade operating with closed processes-based V_{sVs} thermal cycles.

Following the corresponding analysis of both case studies, significant results were obtained. These results, derived from this preliminary design study, will be applied to the implementation of the disruptive SSPP prototype operating with real gases as working fluids. This allows for a precise and clear understanding of the issue of generating useful work through expansion, contraction, or both.

Moreover, according to the results, the SSPP composed by a group of power unites where the efficiency of each power unite operating with air as working fluid only approaches a value of the efficiency of 22%, can exceed 100% of the nominal design power under certain conditions, which supposes a flagrant violation of the principle of conservation of energy due to the fact that such disruptive Self-Sustaining Power Plant is enabled to overcome a Perpetual Motion Machine of second kind.

Keywords: cascade coupling, cooling work, contraction work, forced convection transfer, heat recovery, vacuum work.

Nomenclature**Acronyms****description**

CTF	Cooling Transfer Fluid
DAC	Double-Acting Cylinder
DRSAC	Double reciprocating single-acting cylinder
EP	Electric Power
HTF	Heating Transfer Fluid
PMM	Perpetual Motion Machine
PMM	Perpetual Motion Machine
PP	Power Plant: a group of PUs coupled in cascade
PU	Power Unit operating with an optional thermal cycle: V_{sp} or V_{sVs}
PU	Power Unit Machine
RDAC	Reciprocating Double-Acting Cylinder
RIT	Ratio of Isothermal temperatures $[T_1/T_2]$
RSAC	Reciprocating Single-Acting Cylinder
SAC	Single-Acting Cylinder
SEP	Self Electric Power
SFI	Self-Feed Index $[SFI = (\eta_{th} - 100) / 100]$
SKPMM	Second kind Perpetual Motion Machine
SPPP	Self-Powered Power Plant
SSPM	Self-Sustaining Power Machine

SSPP	Self-Sustaining Power Plant
TE	Thermoelectric Energy
TWF	Thermal Working Fluid
Vsp	Closed processes cycle: [Isochoric (V), isentropic(s), isobaric (p)]
VsVs	Closed processes cycle:[Isochoric(V), isentropic(s) Isochoric(V), isentropic(s)]
Symbols/units	description
$p(\text{bar})$	pressure
$q_i(\text{kJ/kg})$	specific heat in
$q_o(\text{kJ/kg})$	specific heat out
$q_{i12}(\text{kJ/kg})$	Input heat to cycle process 1-2
$q_{o31}(\text{kJ/kg})$	Output heat from cycle process 3-1
$q_{o41}(\text{kJ/kg})$	Output heat from cycles process 4-1
$s(\text{kJ/kg-K})$	specific entropy
$T(\text{K})$	temperature
$T_H(\text{K})$	top temperature
$T_L(\text{K})$	bottoming temperature
$u(\text{kJ/kg})$	specific internal energy
$v(\text{m}^3/\text{kg})$	specific volume
$V(\text{m}^3)$	volume
$w(\text{kJ/kg})$	specific work
$w_i(\text{kJ/kg})$	specific work in
$w_o(\text{kJ/kg})$	specific work out
$w_{oexp}(\text{kJ/kg})$	Output expansion work due to previously added heat
$w_{ocont}(\text{kJ/kg})$	Output expansion work due to previously added heat
$w_{oexp23}(\text{kJ/kg})$	Output expansion work w_{o23} due to previously added heat
$w_{ocont41}(\text{kJ/kg})$	Output contraction work w_{o41} due to previously extracted heat
$w_n(\text{kJ/kg})$	Net useful work $(w_{oexp} + w_{ocont}) = (w_{o23} + w_{o41})$
$w_n(\text{kJ/kg})$	Net useful work $(w_{oexp} + w_{ocont}) = (w_{o23} + w_{o41})$
$q_{rec}/\text{PUI}[\text{kJ/kg}]$	Heat recovered from cooling cycles processes
$T_{q_{rec}}/\text{PUI} [\text{K}]$	Temperature of the heat recovered from cooling cycles processes
$TF(\%)$	Heat transfer losses due t heat recovery effectiveness
$LF(\%)$	Losses factor (thermal and mechanical irreversibilities)
$\eta_{th}(\%)$	Cycle thermal efficiency $[w_n/q_i]$

1. Introduction

This research combines two concepts that, despite being well known, have never been considered for the design and development of technically disruptive and highly efficient power plants. Such concepts consist of the well-known vacuum used in both reciprocating and rotary steam engines, which includes Rankine and ORC and thermal cycles strictly composed by isothermal closed thermodynamic processes of both expansion and contraction or a vacuum.

The idea that vacuums or contraction pressure (any pressure lower than atmospheric pressure or lower than the initial or reference pressure of a contraction-based thermal cycle) can be used to perform useful mechanical work in heat engines is an ancient concept. Practical vacuum systems are available for carrying out useful mechanical work using vacuums obtained by cooling a thermal working fluid in several ways. For instance, some vacuum systems undergo a change of state via the condensation of the thermal working fluid (from steam to liquid water), which can be carried out in both open and closed processes.

Open processes correspond to Thomas Savery, Thomas Newcomen, and, later, James Watt engines, in addition to actual Rankine and organic Rankine cycles equipped with ultimate state-of-the-art improvements, which condense steam, contributing to the generation of a vacuum. When steam is cooled inside a Rankine cycle condenser, entropy decreases even at a constant temperature. Due to the generated vacuum, a significant amount of work is produced in addition to the work obtained by steam expansion. This makes it possible to obtain useful mechanical work when entropy decreases.

The fact that useful work is obtained when entropy decreases, which is evident by observation, seems contradictory to the second law of thermodynamics. However, it is the key to achieving a thermal machine that uses a vacuum to carry out useful mechanical work via the thermal contraction of the thermal working fluid. If strictly isothermal expansion and contraction are added to this technique, highly disruptive and efficient thermal machines are achieved.

No relevant advances were made to the use of vacuums to carry out mechanical work until the 16th century. Thomas Savery (1650–1715) [1]; Thomas Newcomen (1664–1729) [2]; and James Watt (1736–1819) [3], made a valuable contribution to the diffusion of steam engines based on vacuums, highlighting Newcomen's atmospheric steam engine types, in which useful mechanical work is performed under vacuums achieved by condensing the expanded steam exhausted from a cylinder. Later, Watt improved the concept of the atmospheric pressure steam engine designed by Newcomen, implementing prototypes equipped with a steam condenser located independently of the actuator cylinder.

In Newcomen and James Watt steam engines [2–3] that operate at atmospheric pressure in the high-pressure zone and with a vacuum in the low-pressure zone, the volumetric zone of the cylinder in contact with the condenser was subjected to a pressure lower than the atmospheric pressure known as a "vacuum." The work obtained in these engines was due to the generation of a vacuum by cooling via heat extraction from the condenser in an open process. The open process of cooling carried out by heat extraction responsible for this vacuum decreases entropy while providing useful mechanical work. This common phenomenon occurs in reciprocating steam engines at constant pressure, constant temperature, and change of state in open process-based transformations.

Based on the above description, the concept of obtaining useful work accompanied by the decrease in entropy can be expressed by the following statement concerning isothermal vacuum-based work: "It is not possible to perform mechanical work by open process-based contraction due to a vacuum without a decrease in entropy" or "The performance of mechanical work by open-process-based contraction due to a vacuum leads to a decrease in entropy." According to this statement, the decrease in entropy is a consequence of cooling only (independent of temperature and pressure).

Experimental validation involves observing that no useful mechanical work is done if the vacuum is eliminated due to a lack of cooling in the condenser because there is no difference in pressure between atmospheric and vacuum, causing the absence of forces between both sides of the piston. This idea is considered in this research work under closed processes to achieve mechanical work by strictly isothermal contraction under closed processes.

Later, Gerald Müller (2013) [4] presented an innovative concept concerning low-temperature-based atmospheric steam engines. The author extended the theory of the atmospheric steam engine operating under a vacuum achieved by heat extraction to show that operation is possible at temperatures between 60 °C and 100 °C, although efficiency is further reduced as the temperature increases.

Similarly, Gerald Müller and George Parker (2015) [5] conducted a series of experiments to assess this theory by including a forced expansion stroke. Recently, the atmospheric steam engine (which implies that useful work is due to the presence of a vacuum) was re-evaluated. According to the authors, the theoretical efficiency of the ideal engine can be increased from 6.5% to 20%.

The use of vacuums in steam engines is the origin of performing useful mechanical work by thermal contraction. While using a vacuum to obtain useful mechanical work in steam engines has been successfully applied for centuries (Savery and Watt steam engines), it has not been possible to develop strictly isothermal processes for efficient commercial industrial applications. However, during the last three decades, some attempts to advance isothermal processes have been made [6–7].

Recently, Vítor Augusto Andreghetto Bortolin et al. (2021) [6] proposed a complete thermodynamic model for the adiabatic and isothermal atmospheric steam cycle that uses real gas data. The model was constructed to accommodate the forced expansion of low-pressure steam. The results show that the adiabatic cycle is more efficient than the isothermal cycle and that the amount of heat needed to keep the expanding steam at a constant temperature is prohibitive for practical applications. Knowlen C. et al. (1997) [7] developed an automotive propulsion concept of an open Rankine cycle that utilizes liquid nitrogen as the working fluid and discussed several means of achieving quasi-isothermal expansion. The authors claim that if sufficient heat input during the expansion process can be realized, then this cryogenic propulsive system will provide greater automotive ranges and lower operating costs than those of electric vehicles currently being considered for mass production.

Ciconardi S. et al. (1999) [8] studied a steam cycle and the effect of flow variation on cycle performance. The authors claim that isothermal expansion with increasing flow decreases cycle efficiency due to the greater condenser losses and the impossibility of fully recovering the available heat at the end of the expansion at high superheated temperatures. In other research, Ciconardi S. et al. (2001) [9] showed that isothermal expansion can achieve high efficiency (up to 70% of HHV) when the waste heat at the turbine outlet is recovered for pre-heating water, hydrogen, and oxygen. Park J.K. et al. (2012) [10] analyzed a quasi-isothermal thermal cycle for its application in an underwater energy storage system. The analysis of the heat transfer cycle confirmed the validity of the quasi-isothermal nature of the design based on water pistons.

Kim Y.M. et al. (2013) [11] reviewed current thermo-electric energy storage (TEES) systems and proposed a novel isothermal TEES system with transcritical CO₂ cycles. For the given efficiencies of the compressor and expander, the maximum round-trip efficiency decreased rapidly with an increase in the back work ratio. The authors showed that the round-trip efficiency of the isothermal TEES system can be increased because it has a lower back work ratio than in the isentropic case.

Meanwhile, Opubo N. et al. (2013) [12] proposed a variant of a thermal engine that uses isothermal expansion to achieve a theoretical efficiency close to the Carnot limit and in which steam generated inside a power cylinder eliminates the need for an external boiler. The device is suitable for slow-moving applications, and preliminary experiments have shown a cycle efficiency of 16% and a high work ratio of 0.997. Later, Opubo N. et al. (2014) [13] reviewed various low-temperature vapor power cycle heat engines with quasi-isothermal expansion using methods to realize the heat transfer. In this experiment, the heat engines took the form of either a Rankine cycle with continuous heat addition during the expansion process or a Stirling cycle with a condensable vapor as the working fluid.

R. Ferreiro et al. [14–17] presented state-of-the-art technologies for thermal cycles that allow operation with closed processes of both thermal expansion and contraction.

Some interesting topics that has been taken into account deals with three disruptive technological challenges that must be overcome to implement efficient power units (PUs) capable of being operated by means of thermal contraction based on a vacuum under closed processes-based adiabatic-isentropic transformations, due to R. Ferreiro et al. [18–20] as well as optionally contraction based on strictly isothermal closed processes. The first challenge is that a thermal machine must be able to operate with the aforementioned thermal cycle (i.e., it must be capable of operating through thermal contraction). The second challenge is that the thermal cycles of a thermal machine must be able to operate with strictly isothermal processes of both thermal expansion and contraction. The third technological challenge is that a thermal machine must be able to develop highly effective forced thermal convection heat transfer media at the transfer rate required by the nominal power of each PU, where every PU is composed of a pair of RDACs equipped with associated heat transfer equipment.

Mentioned contributions were recently followed by advances on power plants composed by groups of power units coupled in cascade where, R. Ferreiro et al. [21–23], in which regenerative expansion-contraction-based cycles Power Plants have been researched.

The present study is focused on improving the efficiency of Power Plants in which instead of using heat regeneration in the PUs, cascade heat recovery is used, thereby achieving absolutely disruptive efficiencies compared to conventional technologies.

2. Background on SPPP technologies

A self-powered power plant (SPPP) comprises a novel power plant architecture based on a second-kind perpetual motion machine (SKPMM), designed to generate more power than it consumes. However, the focus of the study is not on the SKPMM itself.

According to Noether's theorem, which states that "if a transformation of the coordinate system satisfies a certain condition, namely being continuous, then necessarily there is a quantity that is conserved", or in simpler terms, "every continuous symmetry of the action of a physical system with conservative forces has a corresponding conservation law". Based on Noether's theorem, real perpetual motion machines of the first and third kinds, which purport to produce free energy, are impossible due to the constraints imposed by the second law of thermodynamics and its inherent irreversibilities. That is, real perpetual motion machines of the first and third kinds exhibit dissipative forces, making them impossible. This does not apply to real machines for which dissipative forces are inherent.

The energy conversion processes involved are purely mechanical, such as the conversion of kinetic to potential energy or vice versa, which only involve conservative forces. However, real machines of the second kind experience inherent losses (thermo-mechanical losses due to the conversion of a fraction of kinetic energy into heat from non-conservative forces such as friction), in accordance with the second law. The case of SPPPs, as presented in this research work, while adhering to the second law, is distinctly different as they employ a strategy to compensate for and overcome the inherent losses caused by non-conservative or dissipative forces using an innovative and disruptive heat recovery strategy. Through empirical development, it will be demonstrated that a SKPMM not only overcomes the losses inherent to non-conservative forces, including all types of irreversibilities but also generates more free energy than is necessary to operate at nominal load. This defines a true SPPP

This unprecedented machine consists of a cascaded array of power units (PUs), each designed to defy the limitations imposed by the Carnot factor while still adhering to the principles of the second law of thermodynamics. The SPPP is composed of a series of cascaded PUs, where each PU does not necessarily possess the characteristics of a SKPMM—that is, the capacity to surpass or indeed reach 100% of the externally added power. This implies that a group of PUs, each exhibiting a thermal efficiency of less than 100%, can collectively achieve an SPPP whose efficiency exceeds 100%, without violating the first or second laws of thermodynamics.

This peculiar behavior is attributed to the fact that each PU is capable of performing useful mechanical work through the vacuum created by thermal contraction during heat extraction. The heat removed from the cooling system is effectively reclaimed through a strategy based on the cascaded coupling of PUs, where the recovered heat is reintroduced to the first PU in the SPPP sequence. Consequently, a series of PUs connected in cascade, each with an efficiency of less than 80%, can result in an SPPP that produces more energy than it consumes, thereby exhibiting an efficiency greater than 100%. This is possible because nearly half of the work produced by each cascaded power unit is obtained at no cost (free-cost energy) due to the work of cooling contraction. Moreover, this is further enhanced by the efficient cascaded heat recovery strategy in an additive potential mode, where the magnitude is temperature.

In this study, the concept of 'energy' is assumed to be an intrinsic property of nature, characterized by the potential difference between two points of a trajectory within a physical field magnitude. The trajectory of the magnitude under consideration can be described by a continuous, differentiable function. Among such physical magnitudes are, but not limited to, temperature, electrical potential, pressure difference, electric field potential, magnetic field potential, and gravitational field potential. One of the consequences of the second principle of thermodynamics is the 'principle of minimum energy,' which states that physical systems tend to evolve toward lower energy states due to the tendency toward thermodynamic equilibrium. Thus, in a local context, if the energetic system is in equilibrium, its energy is at a minimum—zero useful energy. As a consequence, the only known method to achieve a potential difference—energy—is by adding external energy, such as work or heat, among other available energetic magnitudes.

2.1 Scientific-Technical Keys to Implementing a SSPM

The analysis of the cycles described below aims to underscore the unique characteristics that distinguish them from conventional thermal cycles, particularly in terms of the energy balance related to heat-to-work conversion. These cycles, characterized by performing useful mechanical work through the thermal contraction of the working fluid, exhibit a coherence in energy balance that challenges traditional models.

The proposed machines are designed to perform useful mechanical work via both expansion and contraction of a thermal working fluid within closed processes. This functionality necessitates the use of reciprocating single- or double-acting cylinders, inherently excluding turbines or any rotating machinery that operates under open processes with continuous flow. Consequently, the study concentrates on actuators that employ reciprocating single- and double-acting cylinders.

The classic types of reciprocating cylinders suitable for use as heat-work converters with a thermal working fluid, or thermo-actuators, include:

Reciprocating Single-Acting Cylinder (**RSAC**), as shown in Figure 1(a)

Double Reciprocating Single-Acting Cylinder in Opposition (**DRSAC**), depicted in Figure 1(d)

Reciprocating Double-Acting Cylinder (**RDAC**), illustrated in Figure 4(a)

The thermal cycles proposed for the actuator structures are as follows:

Vsp Cycle, which consists of the following closed processes:

- 1-2 Heat addition at constant volume (1-2)
- 2-3 Expansion performing work at adiabatic-constant entropy (2-3)
- 3-1 Heat extraction at constant pressure (3-1)

VsVs Cycle, comprising the following closed processes:

- 1-2 Heat addition at constant volume (1-2)
- 2-3 Expansion performing work at adiabatic-constant entropy (2-3)
- 3-4 Heat extraction at constant volume (3-4)
- 4-1 Contraction performing work at adiabatic-constant entropy (4-1)

2.2 Architecture of the RSAC

The reciprocating single-acting cylinder (RSAC) is depicted in Figure 1 (a). The objective of this design structure is to convert added heat to useful work. Work is obtained by the force exerted by the pressure of a working fluid on the piston rod in forward direct ion along the piston stroke. To operate such RSAC a thermal cycle must be used. It consists of a sequence of three closed processes denoted as isochoric heat addition at constant volume (V), adiabatic expansion at constant entropy (s) and isobaric heat releasing at constant pressure (p). Thus, the cycle is identified as Vsp cycle, and is represented Figure 1 according to the following diagrams: Figure 1 (b) depicts the T-s diagram and Figure 1 (c) depicts the p-V diagram.

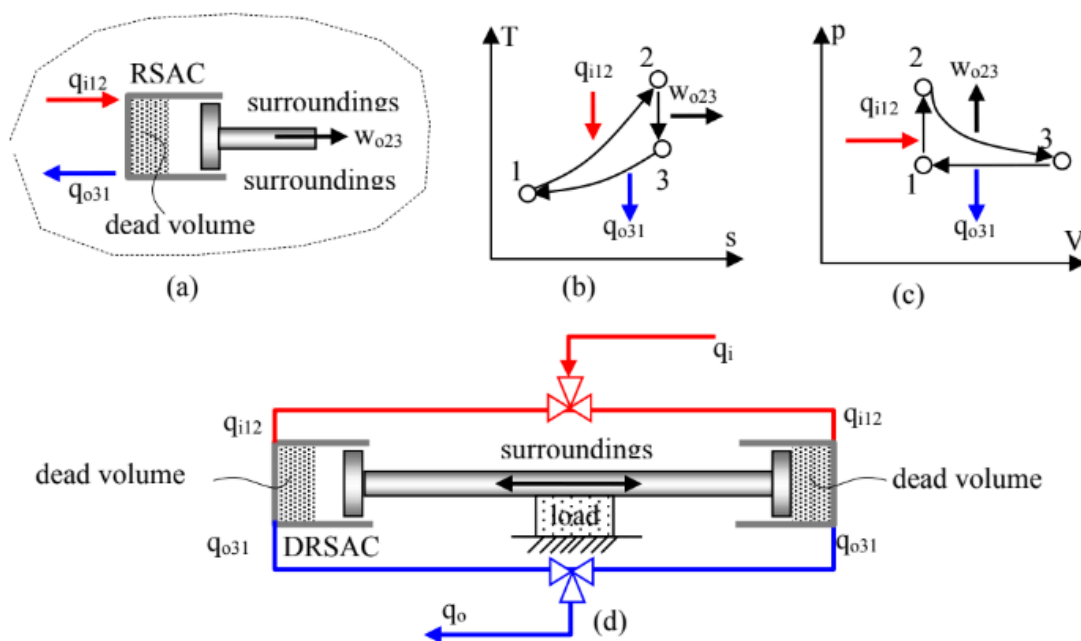


Figure 1: Reciprocating single-acting cylinder (RSAC) and double reciprocating single-acting cylinder (DRSAC) operating with a closed processes-based cycle composed by three transformations carried out by the cycle type Vsp: (a), RSAC structure. (b), T-s diagram. (c), p-V diagram. (d), Double reciprocating single-acting cylinder (DRSAC)

According to a second law statement the added heat cannot be converted totally into work so that an important fraction of the added heat, after the expansion of the working fluid remains in the working fluid as internal energy (low-grade heat) and must be extracted to close the cycle. If such heat cannot be recovered then is loosed to a hat sink. In order to do useful mechanical work along both piston-rod strokes two single-acting actuators are necessary to achieved a double-acting cylinder actuator. This requires simultaneous execution of two single-acting thermal cycles as shown in Figure 1 (d).

Since in the RSAC work is obtained by the force exerted by the pressure of a working fluid on the piston rod in forward direction along the piston stroke, in order to achieve work in both forward and backward strokes an

additional cylinder must be coupled opposed to this one, achieving a DRSAC. With this strategy it is achieved a double-acting actuator. The thermal cycle in each cylinder is executed in such a way that when the left side actuator is in the expansion (advance or forward displacement) phase, the right side actuator is in the contraction (reverse or backwards displacement) phase.

2.3 Vsp cycle transformations

The Vsp cycle depicted in Figure 1 as T-s diagram in (b) and p-V in (c) exhibits a closed process-based isochoric heat addition, a closed process-based adiabatic-isentropic expansion and a closed process-based isobaric heat extraction. The energy balance requires that the difference between input and output heat be equal to the expansion work. That is, fulfils the first law.

The closed processes carried out by the Vsp cycle are depicted in Table 1 and summarized as: 1-2 isochoric heat addition at constant V, 2-3 adiabatic-isentropic expansion at constant s, and 3-1 isobaric compression-based contraction at constant p.

Table 1 Vsp thermal cycle composed of three closed transformations consisting of isochoric heat addition, adiabatic-isentropic expansion while doing mechanical work and isobaric heat releasing.

sp _(i) -sp _(i+1)	Cycle closed processes model	Vsp cycle transformations
1-2	$q_i = q_{i(12)} = u_2 - u_1 = \Delta u_{21} = C_v(T_2 - T_1)$	Isochoric heat addition
2-3	$w_o = w_{o\text{exp}(23)} = u_2 - u_3 = \Delta u_{23} = C_v(T_2 - T_3)$	Adiabatic-isentropic expansion
3-1	$q_o = q_{o\text{cont}(31)} = u_3 - u_1 = \Delta u_{31} = C_v(T_3 - T_1)$	Isobaric heat extraction

2.4 Closed processes-based energy balance on cycle Vsp

The energy balance of the Vsp cycle requires that the input and output energy be equal (energy conservation) or, net heat and net work are equal. Thus, both equalities are modelled as

$$\sum q = \sum w \tag{1}$$

in Eq. (1)

$$\sum q = q_{i12} - q_{o31} \tag{2}$$

$$\sum w = w_o - w_i = w_{o\text{exp}23} \tag{3}$$

Thus, since $w_i = 0$, then $w = w_o = w_{o\text{exp}23}$, so that the energy balance yields

$$q_{i12} - q_{o31} = w_{o\text{exp}23}, \tag{4}$$

or considering that such transformations are carried out under closed processes follows that can be written as

$$\Delta u_{12} - \Delta u_{31} = \Delta u_{23} = w_{o\text{exp}23} \tag{5}$$

2.5 Performance analysis

The thermal efficiency is defined as the ratio of the net work to the net added heat, which can be written as:

$$\eta_{th} = \frac{w_o}{q_i} = \frac{w_{o\text{exp}23}}{q_{i12}} \tag{6}$$

It should be noted that the expression of thermal efficiency for the Vsp cycle does not obey the limitations imposed by the Carnot factor. In fact, the Carnot factor only applies to the cycles of Carnot, Ericsson, and Stirling

(cycles characterized by operating between two constant temperatures commonly denoted as (T_H) and (T_L) or (T_2) and (T_1)).

To illustrate the case under study, a scenario is proposed in which the thermal efficiencies of the Vsp cycle are determined for several thermal working fluids to compare the Carnot factor with the corresponding efficiencies of each thermal working fluid. It will be shown that the Carnot factor is independent of the thermal efficiency of the Vsp cycle for every working fluid.

The results of the cycle computation in terms of performance for carbon dioxide, nitrogen, helium, and hydrogen are shown in Figure 2 and Table 2.

Table 2. Thermal efficiencies and the specific works for the trilateral Vsp cycle operating with several working fluids: carbon dioxide, nitrogen, helium, and hydrogen

$T_2(K)$	CO ₂			N ₂		He		H ₂	
	CF(%)	η (%)	w(kJ/kg)	η (%)	w(kJ/kg)	η (%)	w(kJ/kg)	η (%)	w(kJ/kg)
330	9,09	22,93	4,64	29,54	6,59	41,15	38,46	29,74	91,28
360	16,67	23,40	9,67	30,44	13,59	42,20	78,89	30,59	188,40
450	33,33	24,54	26,81	32,76	36,69	44,91	209,90	32,86	508,50
600	50,00	25,90	60,97	35,77	81,04	48,43	452,70	35,89	1115,00

From the data attained as results of the Vsp cycle computation depicted in Table 2 and Figure 2, it can be highlighted that the fact of converting heat into work undergoing adiabatic path functions is not relevant in terms of thermal efficiency since these parameters are very similar for nitrogen and hydrogen. However, in the case of carbon dioxide and helium, a relevant difference exists: it is lower for carbon dioxide and higher for helium. With regard to the specific work, there are significant differences among the four working fluids considered. For instance, thermal efficiency increases as a function of the thermal working fluid (TWF) ordered as carbon dioxide, nitrogen, hydrogen, and helium. On the other hand, in terms of selection criteria, specific work is relevant in the decision-making task. Therefore, the specific work delivered by the TC operating with hydrogen as TWF, according to Table 2, is significantly greater than when operating with helium. This characteristic is useful to implement a thermal cycle-based engine undergoing the minimum possible weight and size. Nevertheless, if size and weight are not relevant but thermal efficiency is, then helium should be selected as the best working fluid.

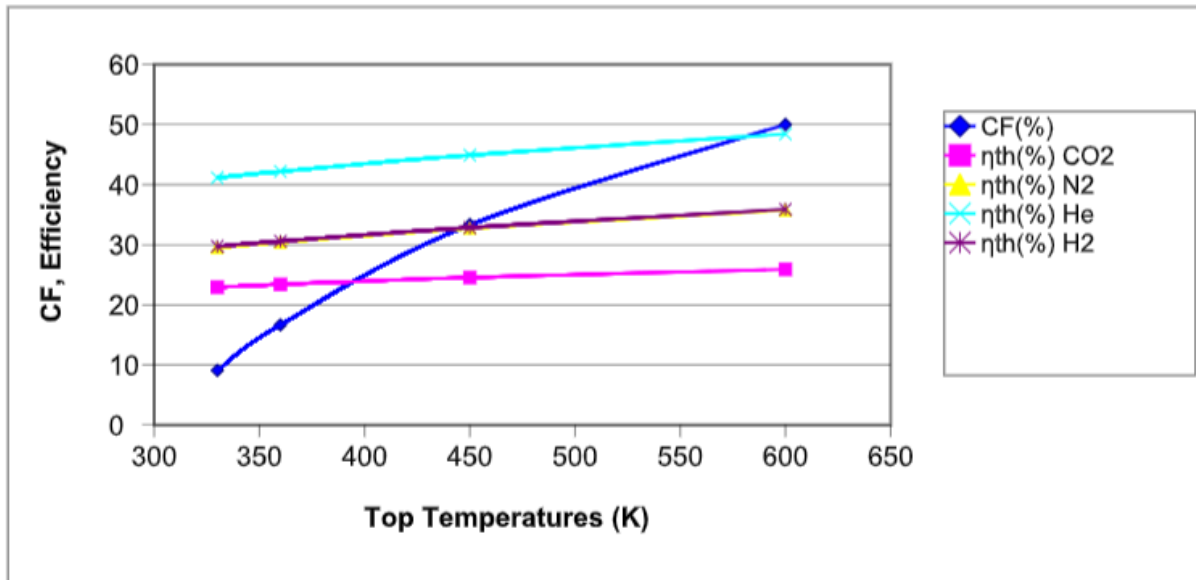


Figure 2: shows the thermal efficiencies of the Vsp cycle for carbon dioxide, nitrogen, helium, and hydrogen as working fluids. The bottom temperature (T_L) is fixed at 300 K, while the top temperatures (T_2) range from 330 to 600 K.

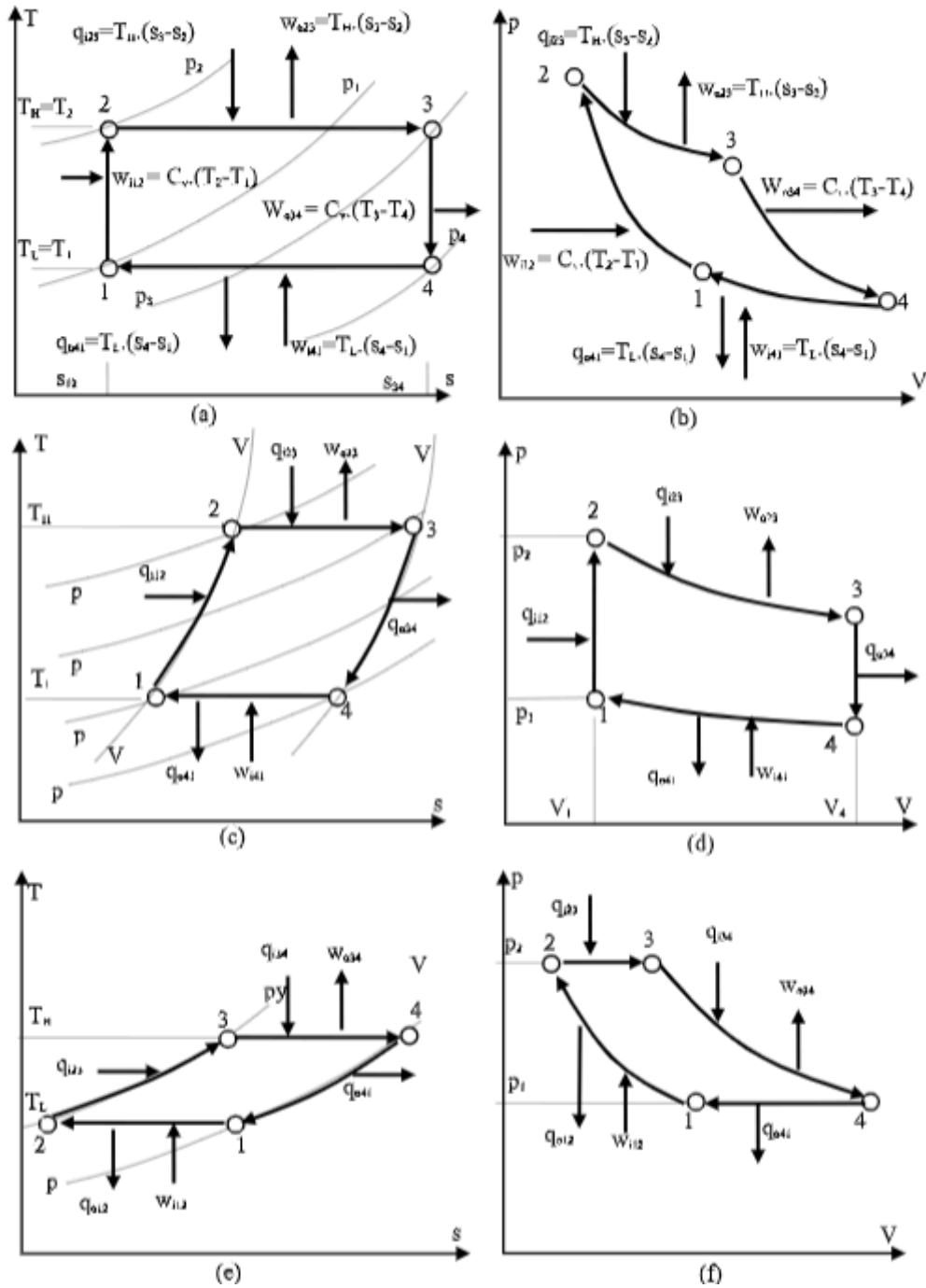


Figure 3: Reversible thermal cycles characterized by obeying Carnot theorem on the basis of operating between two isothermal temperatures.

The Carnot Factor (CF) is compared with the thermal efficiency of the Vsp cycle for each working fluid. As shown in Figure 2, it is observed that for certain lowest top temperatures, CF is lower than the thermal efficiencies of the proposed working fluids, also according to previous research results given in [18-19]. That is, CF is surpassed without violating any fundamental statement related to the first and second laws. In fact, CF, defined as

$$CF = \frac{q_i - q_o}{q_i} = \frac{\Delta s_2 \cdot T_2 - \Delta s_1 \cdot T_1}{\Delta s_2 \cdot T_2} = \frac{\Delta s_2 \cdot \text{isothermal } T_2 - \Delta s_1 \cdot \text{isothermal } T_1}{\Delta s_2 \cdot \text{isothermal } T_2} = \frac{T_2 - T_1}{T_2} = 1 - \frac{T_1}{T_2} \quad (7)$$

is valid for any thermal cycle operating between two (top and bottom) isothermal temperatures such as Carnot, Ericsson, and Stirling cycles. Thus, CF does not establish any limit to the thermal efficiency of any other thermal cycle.

In short, except for thermal cycles operating between two isothermal temperatures:

CF can be surpassed under certain operating conditions according to R. Ferreiro et al. [18-19].

Exceeding the CF does not mean violating any principle of physics.

Table 3 Transformations carried out in the reversible thermal cycles characterized by obeying Carnot theorem on the basis of operating between two isothermal temperatures (T_H and T_L): Carnot cycle, Stirling cycle and Ericsson cycle.

SPs	Cycle transformations
Reversible Carnot cycle. Figure 3 (a) and (b)	
1-2	adiabatic (isentropic) compression
2-3	isothermal expansion and heating at T_H
3-4	adiabatic (isentropic) expansion
4-1	isothermal compression and cooling at T_L
Reversible Stirling cycle. Figure 3 (c) and (d)	
1-2	Isochoric regeneration, internal heat transfer from the working fluid to the regenerator
2-3	Isothermal expansion with heat addition from an external source at T_H
3-4	Isochoric regeneration, internal heat transfer from the regenerator to the working fluid
4-1	Isothermal compression, by absorbing external work with heat rejection to sink at T_L
Reversible Ericsson cycle. Figure 3 (e) and (f)	
1-2	isothermal compression, with heat rejection to the heat sink
2-3	isobaric heating with heat from 4-1 by regeneration,
3-4	isothermal expansion, with heat addition from an external heat source
4-1	isobaric heat transfer by cooling

2.6 Reciprocating single-acting cylinder with contraction-based compression (VsVs)

In Figure 4 it is depicted the reciprocating single-acting cylinder (RSAC) operating with a closed processes-based cycle composed by four transformations: 1-2 isochoric heat addition (heating) at constant V, 2-3 adiabatic-isentropic expansion at constant s, 3-4 isochoric heat extraction (cooling) at constant V, 4-1 adiabatic-isentropic compression-based contraction at constant s, (cycle type VsVs): (a), RSAC structure. (b), T-s diagram. (c), p-V diagram.

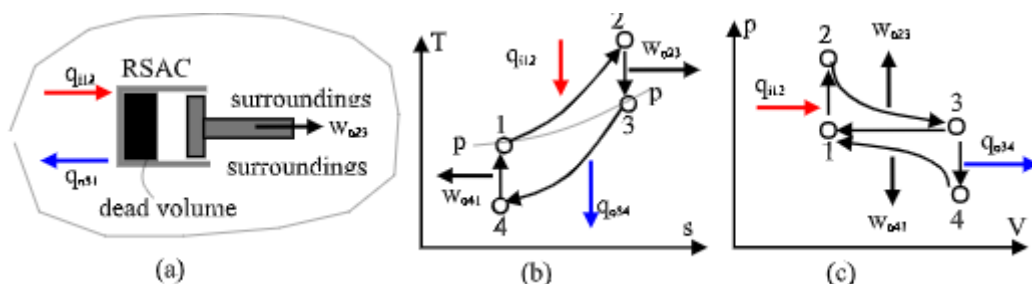


Figure 4: Reciprocating single-acting cylinder (RSAC) operating with a closed processes-based cycle composed by four transformations carried out by the cycle type VsVs: (a), RSAC structure. (b), T-s diagram of the VsVs cycle. (c), p-V diagram of the VsVs cycle.

2.7 VsVs cycle transformations of the RSAC

Table 4 Transformations carried out by the cycle type VsVs.

sp _(i) -sp _(i+1)	Closed processes models	VsVs Cycle Transformations
--	-------------------------	----------------------------

1-2	$q_i = q_{i12} = u_2 - u_1 = Cv(T_2 - T_1)$	Isochoric heat addition
2-3	$w_o = w_{o\text{exp}23} = u_2 - u_3 = Cv(T_2 - T_3)$	Adiabatic-isentropic expansion
3-4	$q_o = q_{o34} = u_3 - u_4 = Cv(T_3 - T_4)$	Isochoric heat extraction
4-1	$w_o = w_{o\text{cont}41} = u_1 - u_4 = Cv(T_1 - T_4)$	Adiabatic-isentropic contraction

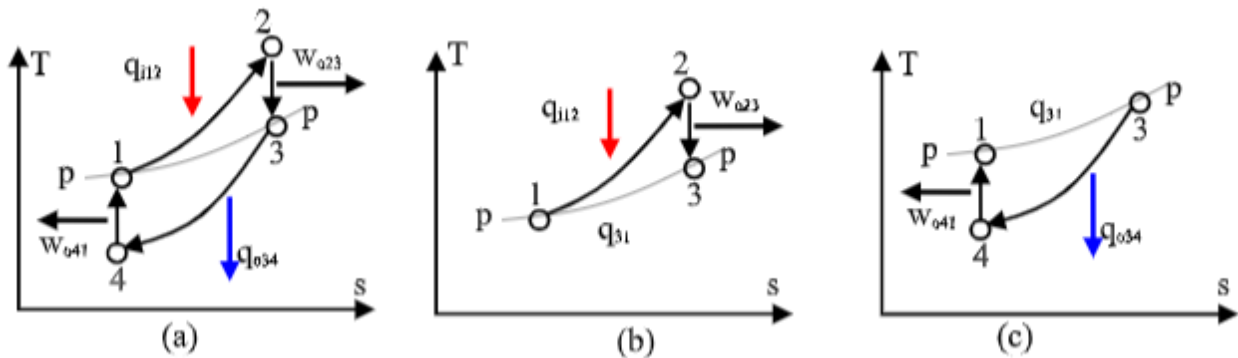


Figure 5: Energy scheduling in the VsVs cycle in two energy balances: the closed processes 1-2, 2-3 and remaining heat 3-1; and the closed processes 3-4, 4-1 and remaining heat 3-1. In this energy balance it is assumed that useful work is done by adding heat and by extracting heat.

As described in Table 4 Figure 3(c) and Figure 5 (c), the closed process 4-1 exhibits the property of increasing internal energy while doing useful mechanical work.

Thus, the RSAC does useful work by means of:

- adding heat to the unique actuator chamber in closed process 1-2
- extracting heat from the unique actuator chamber in closed process 3-4

Heat-work conversion obeys the following sequence:

- isochoric addition of heat prior to expansion in process 1-2

$$q_{i12} = Cv(T_2 - T_1) \tag{8}$$

Doing useful expansion work in process 2-3

$$w_{o23} = w_{o\text{exp}} = Cv(T_2 - T_3) \tag{9}$$

- isochoric extraction of heat in process 3-4

$$q_{o34} = Cv(T_3 - T_4) \tag{10}$$

Doing useful contraction work in process 4-1

$$w_{o41} = w_{o\text{cont}} = Cv(T_4 - T_1) \tag{11}$$

Note that the transformation 4-1 is characterized by:

- increase internal energy while doing useful mechanical work, according to

$$\Delta u_{41} = Cv(T_1 - T_4) \tag{12}$$

which does useful work equivalent to the change in internal energy according to Eq.(13) as

$$w_{o41} = w_{ocont41} = \Delta u_{41} = Cv(T_1 - T_4) \quad (13)$$

Performing useful work while internal energy increases adiabatically (without adding or extracting heat) represents a remarkable achievement (R. Ferreiro [20], 2023). This scenario, previously unprecedented, lacks any references to its application prior to the contribution based on work done through contraction. Consequently, we must introduce necessary modifications to accurately represent the conversion of heat to work.

If the pressure at the beginning of the cycle (reference pressure to as p_{ref}) equals atmospheric pressure, then the work done is exclusively due to two processes:

1 Adding heat (isochoric heating of the working fluid): This process increases temperature and pressure, followed by an adiabatic-isentropic expansion while performing useful work.

2 Extracting heat (isochoric cooling of the working fluid): Responsible for decreasing temperature and pressure (creating a vacuum), this process is followed by an adiabatic-isentropic contraction while performing useful work.

In summary, within the VsVs cycle operating in a RSAC, the remaining heat q_{31} is utilized to balance the energy associated with two modes of mechanical work:

1 Expansion work (w_{o23}), resulting from the heat added (q_{i12}).

2 Contraction work (w_{o41}), arising from the heat extracted (q_{o34}).

2.8 Closed processes-based energy balance in the VsVs cycle of a RSAC

Taking into account the input and output heats, which are heating and cooling heats also known as added and extracted heats, follows that:

$$q_i = q_{i12} \quad (14)$$

$$q_o = q_{o34} \quad (15)$$

It is obvious that

$$q_{i12} - q_{o34} \neq w_o \quad (16)$$

which means that

$$\sum q \neq \sum w \quad (17)$$

Does the result of Eq. (17) violate the first principle?

According to T-s diagram in figure 3(a) and (b) the amount of heat confined into the closed volume of the cylinder chamber is the remaining heat after the expansion

$$q_{31} = u_3 - u_1 = \Delta u_{31} \quad (18)$$

Thus, the response to adding heat to the fraction of the VsVs cycle doing work by expansion according Figure 3(b), is

$$q_{i12} = w_{o\text{exp}23} + q_{31} \quad (19)$$

Such remaining heat q_{31} will be utilized to generate vacuum by means of heat extraction by cooling the working fluid, where q_{31} is the released heat or the heat that cannot be converted to work as stated by the second law.

Such remaining heat q_{31} is supported by the working fluid confined into the closed volume of the cylinder chamber. Thus, the useful work due to adding heat is:

$$w_{o\text{exp}23} = q_{i12} - q_{31} \quad (20)$$

According to T-s diagram in figure 3(a) and (c)

$$q_{31} = u_3 - u_1 = \Delta u_{31} \quad (21)$$

Considering the fraction of the VsVs cycle doing work by contraction-based compression due to heat extraction according Figure 3(c), follows that the response to extracting heat is:

$$q_{o34} = w_{ocont41} + q_{31} \quad (22)$$

where q_{31} is the released heat or heat that cannot be converted to work as stated by second law. Such remaining heat q_{31} is supported by the working fluid confined into the closed volume of the cylinder chamber. Thus the useful work due to extracting heat is

$$w_{ocont41} = q_{o34} - q_{31} \quad (23)$$

The work described by Eq. (23) is obtained at free cost.

Since there is not heat transfer to the cycle but cycle heat absorption implies that the first law is not violated. Consequently, the net useful work is:

$$w_o = w_{oexp23} + w_{ocont41} \quad (24)$$

instead of $w_o = q_{i12} - q_{o34}$, since $w_o \neq q_{i12} - q_{o34}$

From Eq. (24), some relevant information can be deduced about the behaviour of thermal efficiency with respect to thermal cycles that are not enabled to perform mechanical work by thermal contraction. That is, there is an essential difference in terms of thermal efficiency between thermal cycles without contraction such as the Vsp cycle and cycles that operate with contraction such as the VsVs cycle.

While thermal cycles without contraction exhibit a thermal efficiency that is a function of the top or maximum temperature of the cycle, the thermal efficiency of cycles that operate with thermal contraction is very little dependent on the maximum temperature of the cycle and instead is very dependent on the minimum temperature.

The effect of doing work by contraction due to cooling by heat extraction affects the efficiency of the thermal cycle VsVs in that the efficiency of the cycle at high top temperatures is almost similar to the efficiency at low top temperatures. That is, it has little dependence on the temperatures of the power supply.

We must take into account that during the energy balance of the VsVs cycle, the principle of conservation of energy for closed processes has not been violated. Thus, the relationship between energy balances for closed processes-based heat-work interactions in the VsVs cycle include the following balance models:

From Eq. (20),

$$q_{i12} = w_{oexp23} + q_{31} = Cv(T_2 - T_3) + q_{31} \quad (25)$$

From Eq. (23),

$$q_{o34} = w_{ocont14} + q_{31} = Cv(T_1 - T_4) + q_{31} \quad (26)$$

thus, in order to find the relationship between heat and works, we proceed by eliminating the factor q_{31} from both equations (25) and (26) according to:

$$q_{i12} - w_{oexp23} = q_{o34} - w_{ocont14} \quad (27)$$

Which yields

$$w_{oexp23} - w_{ocont14} = q_{i12} - q_{o34} \quad (28)$$

Thus, since the total useful work w_o is $w_{o\text{exp}23} + w_{o\text{cont}14}$, follows that from Eq. (28) the amount of heat transferred to/from the VsVs cycle to achieve the work w_o is:

$$w_{o\text{exp}23} - w_{o\text{cont}14} + 2 \cdot w_{o\text{cont}14} = q_{i12} - q_{o34} + 2 \cdot w_{o\text{cont}14}$$

Which, once simplified, yields

$$w_o = w_{o\text{exp}23} + w_{o\text{cont}14} = q_{i12} - q_{o34} + 2 \cdot w_{o\text{cont}14} \tag{29}$$

From Eq. (29) the rejected heat q_{o34} towards the heat sink of every VsVs cycle is obtained as:

$$q_{o34} = q_{i12} - w_o + 2 \cdot w_{o\text{cont}14} \tag{30}$$

The amount of heat q_{o34} is important since it is responsible for supplying heat energy to the next downstream

PU's coupled in cascade. Therefore, the heat q_{o34} rejected by the VsVs cycle, instead of being conducted to a thermal sink, will be recovered to feed the next downstream power unit until completing a self-powered thermoelectric plant.

2.9 Performance analysis

The achieved enhancement obey the fact that if the thermal efficiency due to expansion work is the ratio of the added heat to the achieved work by expansion as

$$\eta_{th(\text{exp})} = \frac{w_{o\text{exp}23}}{q_{i12}} \tag{31}$$

and the thermal efficiency due to contraction work is the ratio of the work out due to cooling heat to the cooling heat

$$\eta_{th(\text{cont})} = \frac{w_{o\text{cont}14}}{q_{o34}} \tag{32}$$

the thermal efficiency due to both output works (expansion plus contraction) works is the ratio of the net useful work due to expansion and contraction to the added heat

$$\eta_{th} = \eta_{th(\text{exp+cont})} = \frac{w_{o\text{exp}23} + w_{o\text{cont}14}}{q_{i12}} \tag{33}$$

However,

$$\eta_{th} \neq [\eta_{th(\text{exp})} + \eta_{th(\text{cont})}] \text{ means that } \eta_{th} \neq \left[\frac{w_{o\text{exp}23}}{q_{i12}} + \frac{w_{o\text{cont}14}}{q_{o34}} \right] \tag{34}$$

So, since the numerators in equations (31) and (32) are positive quantities, follows that (33) is greater than (31). That is:

$$\eta_{th(\text{exp+cont})} > \eta_{th(\text{exp})} \tag{35}$$

This means that the thermal efficiency of a thermal cycle delivering useful mechanical work achieved by expansion plus contraction, inherently free of costs, is superior to that of any thermal cycle that only performs mechanical work by thermal expansion.

Along the above analysis, performance behaviour which is inherent to the nature of heat-work conversion techniques applied to contraction-based cycles, the following considerations have been assumed:

- 1 Heat to mechanical work: $CF < \text{efficiency} < 100\%$
- 2 Mechanical work to heat conversion via friction: 100% efficient
- 3 Mechanical work to heat conversion via electric power: $\text{efficiency} < 100\%$

Throughout the thermal efficiency analysis, the principle of energy conservation has not been violated.

2.10 The reciprocating double-acting cylinder (RDAC) actuating into both cylinder chambers A and B

The thermo-actuator based on the double-acting cylinder exhibits the advantageous characteristic of performing double work per cycle at the cost of using double the amount of heat. This allows increasing the power/weight ratio of the mechanical structure of the heat engine. Such structure is depicted in Figure 6.

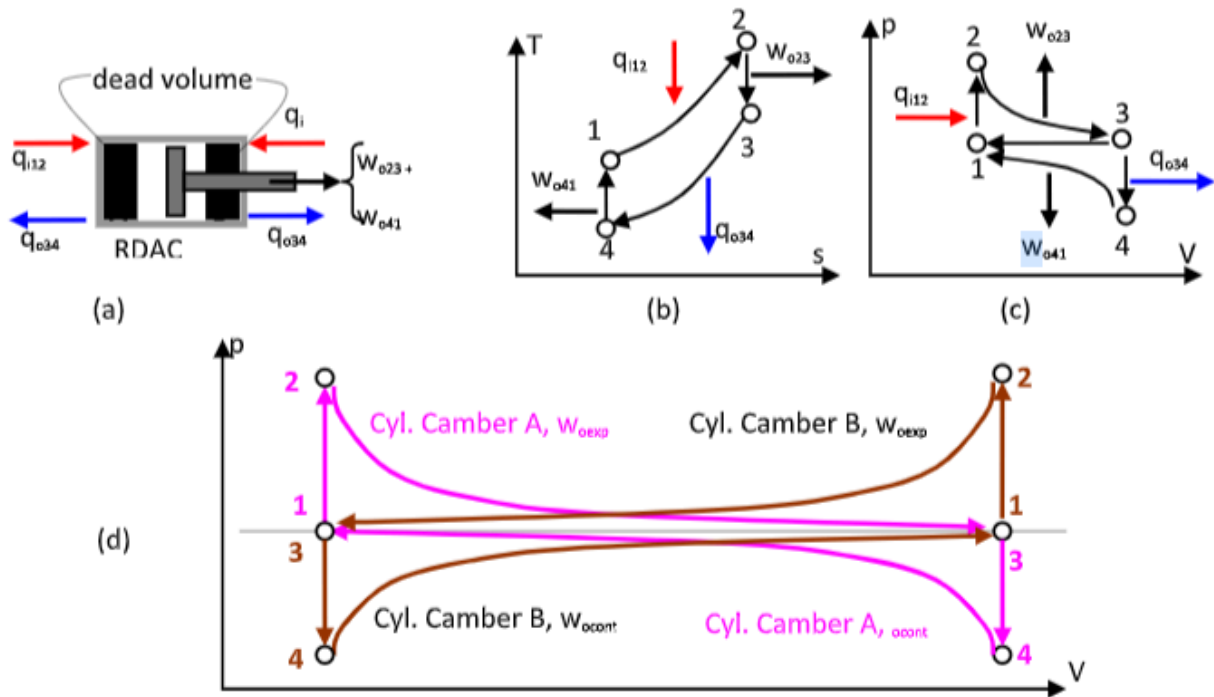


Figure 6: RDAC operating with a closed processes-based double-VsVs cycle as represented in Table 5. (a): RDAC, (b): T-s diagram of the VsVs cycle. (c): p-V diagram of the VsVs cycle. (d): double p-V cycle of the type VsVs operating simultaneously on both cylinder chambers.

The thermo-actuator and cycle depicted in Figure 6 corresponds to a RDAC operating with a closed processes-based VsVs cycle simultaneously in both cylinder chambers A and B. It is composed by four transformations: 1-2 isochoric heat addition (heating) at constant V, 2-3 adiabatic-isentropic expansion at constant s, 3-4 isochoric heat extraction (cooling) at constant V, 4-1 adiabatic isentropic compression-based contraction at constant s, (cycle type VsVs): (a), RDAC structure. (b), T-s diagram. (c), p-V diagram.

Comparing the processes shown in Table 5, it is observed that there is a lag between the VsVs cycles carried out simultaneously in chambers A and B of the reciprocating double-acting cylinder. This means that when expansion takes place in chamber A of the cylinder, contraction takes place in chamber B. Likewise, when heat is added to chamber A, heat is extracted from chamber B.

Table 5 Double VsVs cycle transformations operating simultaneously on both cylinder chambers A and B. The p-V diagram of the simultaneous VsVs cycles is depicted in Figure 5 (d)

cylinder chamber (A)			cylinder chamber (B)		
$sp_{(i)}-sp_{(i+1)}$	Closed process	Const.	$sp_{(i)}-sp_{(i-1)}$	Closed process	Const.
1-2	$q_i = q_{i12} = \Delta u_{12}$	V	3-4	$q_o = q_{o34} = \Delta u_{34}$	V

2-3	$w_o = w_{o\text{exp}23} = \Delta u_{23}$	s	4-1	$w_o = w_{o\text{cont}41} = \Delta u_{14}$	s
3-4	$q_o = q_{o34} = \Delta u_{34}$	V	1-2	$q_i = q_{i12} = \Delta u_{12}$	V
4-1	$w_o = w_{o\text{cont}14} = \Delta u_{14}$	s	2-3	$w_o = w_{o\text{exp}23} = \Delta u_{23}$	s

2.11 Remarkable Thermodynamic Properties of the VsVs Cycle

The ideal VsVs thermal cycle, depicted in Figures 5(a) and 6(b), exhibits certain thermodynamic properties in terms of the relationships between the ranges of isochoric heating and cooling temperatures. This relationship is useful to assess the maximum and minimum temperature ranges, expressed in terms of the ratio defined as T_1/T_2 , in order to achieve an acceptable cycle efficiency.

Therefore, to efficiently utilize the available heat—both added and extracted—it is necessary to understand the relationships between the heats transferred (adding and extracting heat) and the associated mechanical work, as well as the temperatures between which it is possible to achieve acceptable efficiencies. The following analysis addresses this topic. Assuming that the work obtained by contraction due to previously extracted heat is acquired without cost, it is advantageous to use the cooling potential as much as possible to maximize the amount of work. This is achieved by cooling the thermal working fluid relative to the work of expansion carried out by the prior addition of heat, which incurs costs.

To define the ratio of **isochoric low to high temperatures**, $RIT = T_1/T_2$, let's transform the work equations from Table 5 according to the following expressions: From

from $w_{o\text{exp}23} = Cv(T_2 - T_3)$ we have

$$Cv \cdot T_2 = w_{o\text{exp}23} + Cv \cdot T_3 \quad (36)$$

and from $w_{o\text{cont}14} = Cv(T_1 - T_4)$ we have

$$Cv \cdot T_1 = w_{o\text{cont}14} + Cv \cdot T_4 \quad (37)$$

The appropriate combination of Eq. (36) and (37) allows us to express the RIT as a function of the mechanical works

$$RIT = \frac{T_1}{T_2} = \frac{w_{o\text{cont}14} + Cv \cdot T_4}{w_{o\text{exp}23} + Cv \cdot T_3} \quad (38)$$

Since the RIT reaches its maximum value when the temperatures are equal, that is, when the numerator and the denominator of Eq. (38) are equal, this requires that for $T_1 = T_2$ then:

$$w_{o23} + Cv \cdot T_3 = w_{o14} + Cv \cdot T_4 \quad (39)$$

From Eq. (39), it is deduced that under this condition, the work achieved by contraction approaches the work achieved by expansion, which approaches the maximum achievable thermal efficiency. However, real systems are subject to all types of irreversibilities due to the inherent interaction of non-conservative forces. Since the maximum value of the RIT occurs for $T_1 = T_2$, the desired value of the RIT is the one that allows obtaining the greatest efficiency in a range of real power units, typically found in the range of values between 0.80 and 0.95. A high RIT value will require a larger number of cascaded Power Units (PUs), while a lower RIT value will require fewer PUs to complete a self-powered power plant. Consequently, the next step involves the prototyping description task, in which the concept of RIT will be applied as a cycle efficiency enhancement criterion.

In summary, it is important to highlight that the studies conducted in this section, including both the actuating mechanisms based on reciprocating double-acting cylinders and their associated thermal cycles, have complied with thermodynamic principles. These mechanisms are characterized by providing useful mechanical work through the contraction of the thermal working fluid or by creating a vacuum. It has been demonstrated that

neither the first principle of thermodynamics (conservation of energy) nor the second principle (as stated by Clausius and Kelvin-Planck) has been violated.

3 The self-powered power plant (SPPP) design task

3.1 Background of perpetual motion machines (PMM)

Perpetual motion machines of the first and third kinds are characterized by their ability to do work indefinitely without an external energy input. This is based on the law of energy conservation while also satisfying Noether's theorem. Ideally, such machines would be possible; however, their actual implementation is not. Real machines will exhibit inherent irreversibilities (losses) derived from dissipative forces, such as friction.

On the other hand, perpetual motion machines of the second kind, whose operation mode consists of a combination of mechanical and thermal transformations, are inherently affected by dissipative forces. These include irreversibilities due to mechanical losses primarily from friction, sound energy, as well as thermal losses including isentropic losses due to flow work caused by the thermal fluid friction, heat leaks, and heat transfer losses (due to conduction, convection, and radiation). Accordingly, does not satisfy Noether's theorem. As consequence, according to the second law of thermodynamics (Clausius and Kelvin-Planck statements), such a perpetual motion engine is impossible.

However, nature exhibits some cases in which this type of engine is possible as an inherent mode of behavior. This is the case with atomic electrons, which do not cease their dynamics, overcoming the resistance of neighboring electrons as well as the attractive force of the nucleus, even when they are in a state of zero-point energy. It is also the case with the dynamics of the cosmos, where, from eternity, its activity does not cease, overcoming all the irreversibility inherent to its existence.

In summary, the second kind of perpetual motion machine is inherent to nature, making it theoretically possible. So, based on the fact that nature makes perpetual motion machines of the second type work correctly, as researchers we are obliged to try to discover at least how it does it and try to replicate its example.

3.2 The strategy for overcoming resistance to achieve self-sustaining engines (SSEs)

This phase of the SSE description addresses the prototype design and implementation task. It focuses on providing more useful work than the heat required by the system. This implies that the thermal efficiency of the SSE would be greater than 100%. However, in compliance with the first and second laws of thermodynamics, the thermal efficiency of any individual power unit according to some results of analysis of VsVs cycles exhibits a thermal efficiency of less than 60% when air is used as the working fluid and less than 80% when helium is used as the working fluid.

The studied thermal cycles, which enable the performance of useful mechanical work through thermal contraction or vacuum, are characterized by their efficiency exceeding the Carnot factor (CF) under certain cycle conditions in such a way that:

- 1 $CF < \text{efficiency} < \text{upper limit of thermal efficiency}$
- 2 For air as the thermal working fluid, $CF < \text{efficiency} < 60\%$
- 3 For helium as the thermal working fluid, $CF < \text{efficiency} < 80\%$

These thermal cycles, characterized by efficiencies exceeding the CF, are attributed to certain key factors that are crucial for improvement:

Key factors for the efficiency enhancements in individual power units (PUs):

- 1 Closed processes-based thermal cycles, as opposed to open processes.
- 2 Absence of state changes in the transformations within a closed cycle.
- 3 Cycles equipped with the necessary apparatus to perform contraction-based work achieved through cooling.

The development and implementation of thermoelectric plants, characterized by generating more power than they consume for operation, are absolutely disruptive in terms of thermal energy utilization. They fundamentally consist of a set of PUs connected in cascade, each equipped with special thermal energy management capabilities. The fundamental characteristic is that a set of power units connected in thermal cascade, where each PU operates with an efficiency of less than 80% when using helium, and less than 60% when using air, can be implemented in such a way that the net useful work is greater than the heat supplied to the first PU in the group. This results in a self-powered thermoelectric plant (SPPT). To achieve such a disruptive effect, a series of key constructive and operational factors must be met:

Essential Key Factors to Achieve Self-Powered Power Plants (SPPPs):

- 1 A unified heat carrier circuit for cascaded Power Units (PUs) responsible for both adding and recovering heat efficiently.
- 2 A reduced Ratio of Isochoric Temperatures (RIT) to enhance the efficiency of each individual PU.
- 3 The task of supplying heat to the top PU in the cascade coupling structure is carried out using one of the available heat transfer techniques based on heat overlay using the thermal energy superposition potential technique which consists in adding heat by increasing temperature.

3.3 Description of the proposed PU structure

A discontinuous motion power unit prototype characterized by the need for two RDACs which do not need any feed pump or reservoir of working fluid for alternating the processes of isochoric heating and cooling. Each cylinder is equipped with dead volumetric reservoirs located in both cylinder chambers according to Figure 7. A relevant issue concerning to any power plant according Figure 7 is the heat transfer equipment. Taking this into account, efforts to find realizable strategies to avoid heat transfer losses is a priority and therefore must be considered. Among the options available for supplying heat to the top cascade PU under conventional mode are combustion chamber-based boilers, which are characterized by high temperature (HT). Other sources include HT-based concentrated solar heat, HT-based nuclear heat, and heat recovered from the Brayton cycle evacuation in combined cycles, which is characterized by medium temperature (MT). Additionally, there are some low-grade heat sources. However, these heat recovery techniques cannot be utilized due to their lack of effectiveness.

A detailed design description is presented in the patent with application number P202200035. Since this prototype is self-sustained none of the mentioned power supply techniques will be used. However, based on the fact that the proposed machine is composed by individual PUs coupled in cascade, it exhibits high efficiency even at medium and low temperatures, so that it is ideal for efficiently recovering the heat evacuated by the cascaded power units upstream. Therefore, for an efficient heat recovery task, effective recovery exchangers (HREs) will be required. During the last three decades, a great effort has been made to implement highly effective heat recovery units. For this reason, there is an abundant bibliography where advanced design techniques are shown, particularly recently, highlighting the work of Sharma and Singh[26] who considered the physical parameters of a HRSG to study their implications on HRSG design by comparing the existing plant design with an optimized plant design, as well as Sharma and Singh[27] who presented the exergy analysis of a HRSG for calculating exergy losses, heat transfer, and pressure losses for different physical components, finding that various subsections of HRSG having different physical parameters like fin density, fin thickness, fin height, tube diameter, and fin spacing show a noticeable effect on exergy loss minimization.

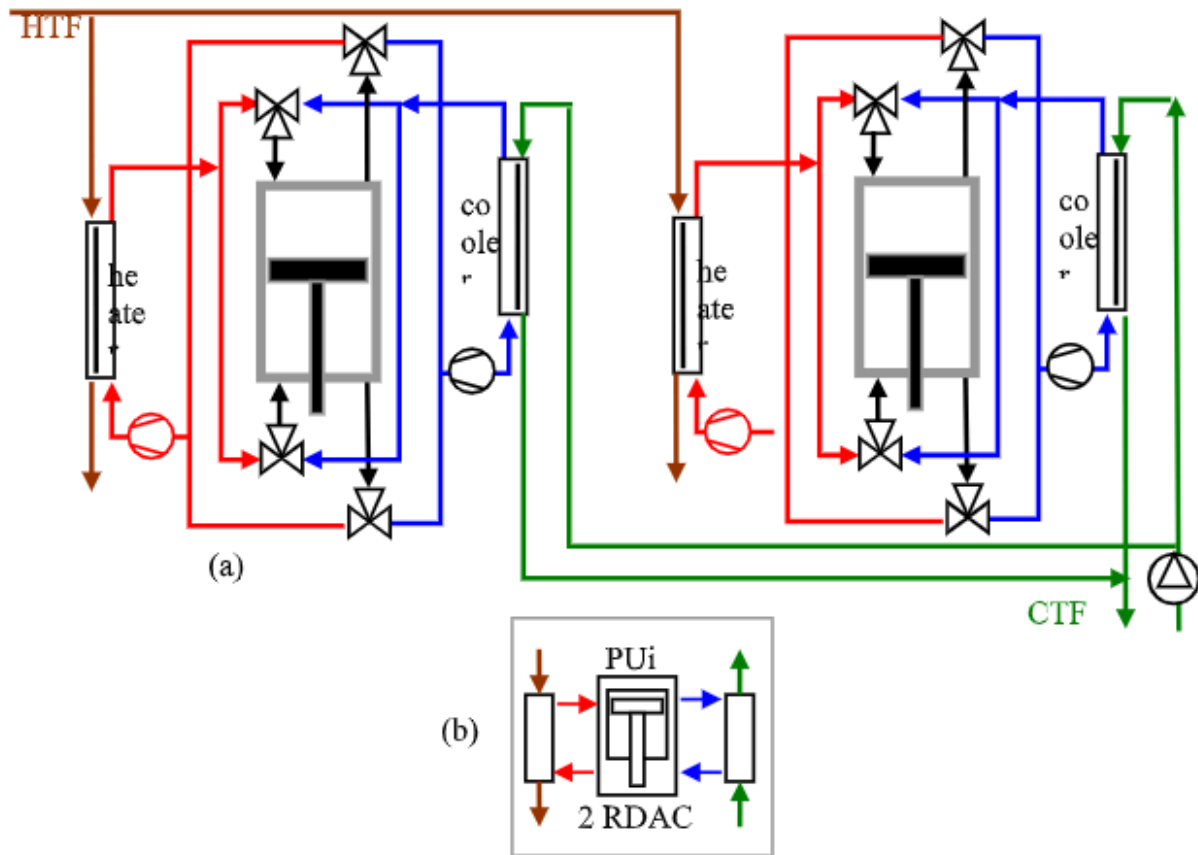


Figure 7: Power unit equipped with two discontinuous RDACs in order to achieve a continuous motion device-based power unit. (a): two discontinuous RDACs structure. (b): Symbol assumed for the above RDAC-based power unit. The design is based on the patent with application number P202200035 and publication number ES-2956342 A2.

Consequently, such information is of use in the design of new HRSG technologies and useful to reduce the thermal losses in existing HRSGs. Furthermore, such design strategies and advanced methodologies could be applied on the designing tasks of HREs to achieve more effective prototypes in terms of heat transfer effectiveness.

In Figure 7 it can be seen that each RDAC has four circuits: two for heat addition (brown and red) and two for heat extraction (green and blue). The heating heat transfer fluid (HTF in brown) is responsible for providing heat to the thermal working fluid (TWF in red). The administration of heat to both chambers of the RDAC is carried out by controlling the corresponding three-way-two-position valves in accordance with the thermal cycle to be executed. In this case, the VsVs thermal cycle described in section 2 has been selected.

The cooling heat transfer fluid (CTF in green) is responsible for extracting heat from the thermal working fluid (TWF in blue). Heat administration from both chambers of the RDAC is carried out by controlling the corresponding three-way-two-position valves in accordance with the thermal cycle to be executed; in this case, the VsVs thermal cycle. To promote heat transfer both to heat and cool the thermal working fluid (TWF), the circulation of the TWF is forced by means of compressors (fans) achieving effective forced convection heat transfer.

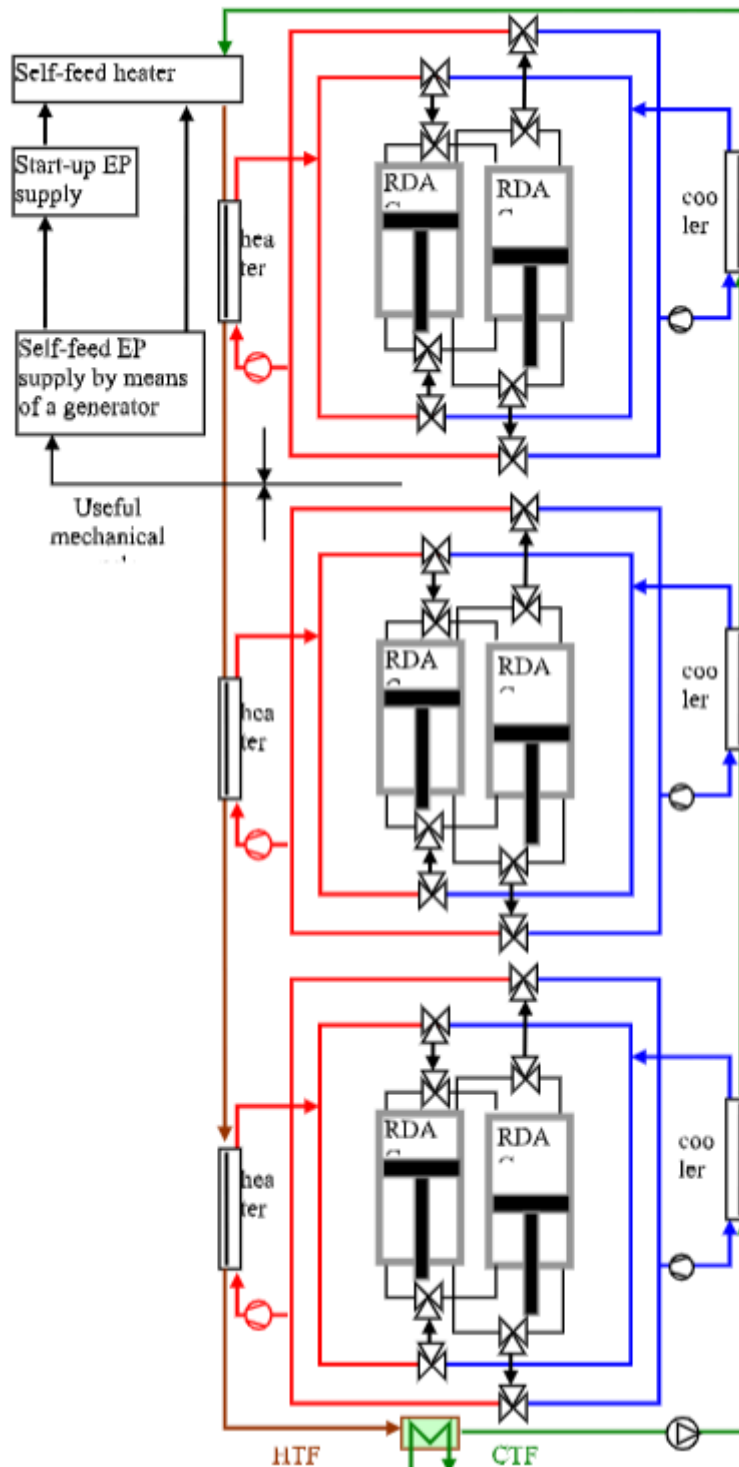


Figure 8: Cascade coupling scheme of a SPPP equipped with three PUs. The design is based on the patent with application number P202200035 and publication number ES-2956342 A2. The details regarding the operating modes of the SSM shown in Figure 8 are found in the patent specification whose design is based on the patent with application number P202200035 and publication number ES-2956342 A2.

In Figure 8 it is depicted a cascade coupling scheme of a SPPP equipped with three PUs. In this figure it can be observed the HTF circuit in brown color along the heating section of pipe and in color green the cooling section of pipe conducting the same fluid operating as CTF. The same HTF is used for both, the heat adding section of heating piping and the heat recovering section of the cooling piping.

Apart from the power units equipped with their heat supply and extraction exchangers, the first power unit is equipped with a heat management system. This system consists of three fundamental components:

- 1 Heat exchanger (Self-feed heater) responsible for increasing the temperature of the heat transfer fluid to supply heat to the cascaded downward power units,
- 2 Electrical energy accumulation system (Star-up EP supply) to provide electrical energy to the heat exchanger described in 1 during the start-up phase.
- 3 Electrical network (Star-up EP supply) from which electrical energy is supplied to the external network as well as to the first power unit of the installation described.

Likewise, it also needs a thermal sink responsible for cooling the HTF to the ambient temperature or minimum temperature to which the TWf of the first upstream PU has to be cooled. Located immediately after the upstream thermal sink, is a HTF recirculation pump. The first function performed by the HTF when driven by the pump is to cool the cascade of upstream PUs, recovering the cooling heat to transfer it to the first PU that operates at the highest temperature in the installation. One of the fundamental keys to achieving enhanced efficiency is based on the fact that the greater the amount of heat recovered, the lower the amount of heat that needs to be supplied to the first PU.

All isolated real thermal cycles must comply with the first and second laws of thermodynamics and therefore adhere to Noether's main theorem. However, the cascade coupling strategy of thermal cycles, which individually comply with the first and second laws, can surpass the limits set by these fundamental principles and generate more energy than they consume, thus functioning indefinitely.

To achieve this, they must satisfy three currently feasible conditions:

- 1 A cascade heat recovery strategy (without heat regeneration).

The conversion of nearly 100% of work into heat –electrical energy to heat– using one of the three available techniques referenced in (4) which are characterized by transferring heat by superposition of heat potential such as:

- a) Infrared-based radiation by means of electric resistance heating, or
- b) Microwave-based heating, or
- c) Magnetic induction-based heating.

- 2 Additionally, another technique is available to convert work into heat that exhibits an efficiency of 100%: it consists of a dissipative magnitude such as resistance to movement in both liquid and gaseous fluids (drag) and mechanical friction (friction).

A heat scheduling strategy is proposed that utilizes the cooling heat from each preceding PU upward to supply heat to the first PU by means of the power supply. Consequently, the heat supplied to the next PU downward is divided into two energy fractions: one that is directly converted into work and the complementary fraction of heat that is used to power the next downward PU. Based on the heat power supply strategy to the first PU, the breakthrough disruptive characteristic lies in the fact that the Self-Powered Power Plant (SPPP) is capable of achieving a thermal efficiency greater than 100% of the heat added to the first PU of an SPPP composed of a series of cascaded PUs, all while adhering to the constraints imposed by the first and second laws of thermodynamics. In other words, the sum of the individual works of each PU within the SPPP exceeds the heat supplied to the first PU of the SPPP. This excess of work obtained is due to the class of thermal contraction, which is free of energy costs, with the condition that there is a coast-free cooling system.

This revolutionary result is attained by capitalizing on the heat recovered from each upstream PU to be reused in powering the first PU; in essence, bolstering the heat input through the heat discharged in each successively coupled PU. The end result is that, with the strategy of scheduling the recovered heat, more useful work is produced than the heat required powering the first PU of the thermoelectric power plant.

This heat management strategy is represented by Figures 9 and 10.

Figure 9 illustrates the HTF recirculation circuit used to feed thermal cycles of the Vsp type. These cycles are not characterized by their ability to provide useful mechanical work through thermal contraction. The absence of this capability means de facto that the thermal efficiency of this cycle is lower than that of any thermal cycle that can perform work through thermal contraction.

Figure 10 illustrates the HTF recirculation circuit used to feed thermal cycles of the VsVs type. These cycles are characterized by their ability to provide useful mechanical work through thermal contraction. This capability de facto, means that the thermal efficiency of this cycle is greater than that of any thermal cycle that can perform work without thermal contraction.

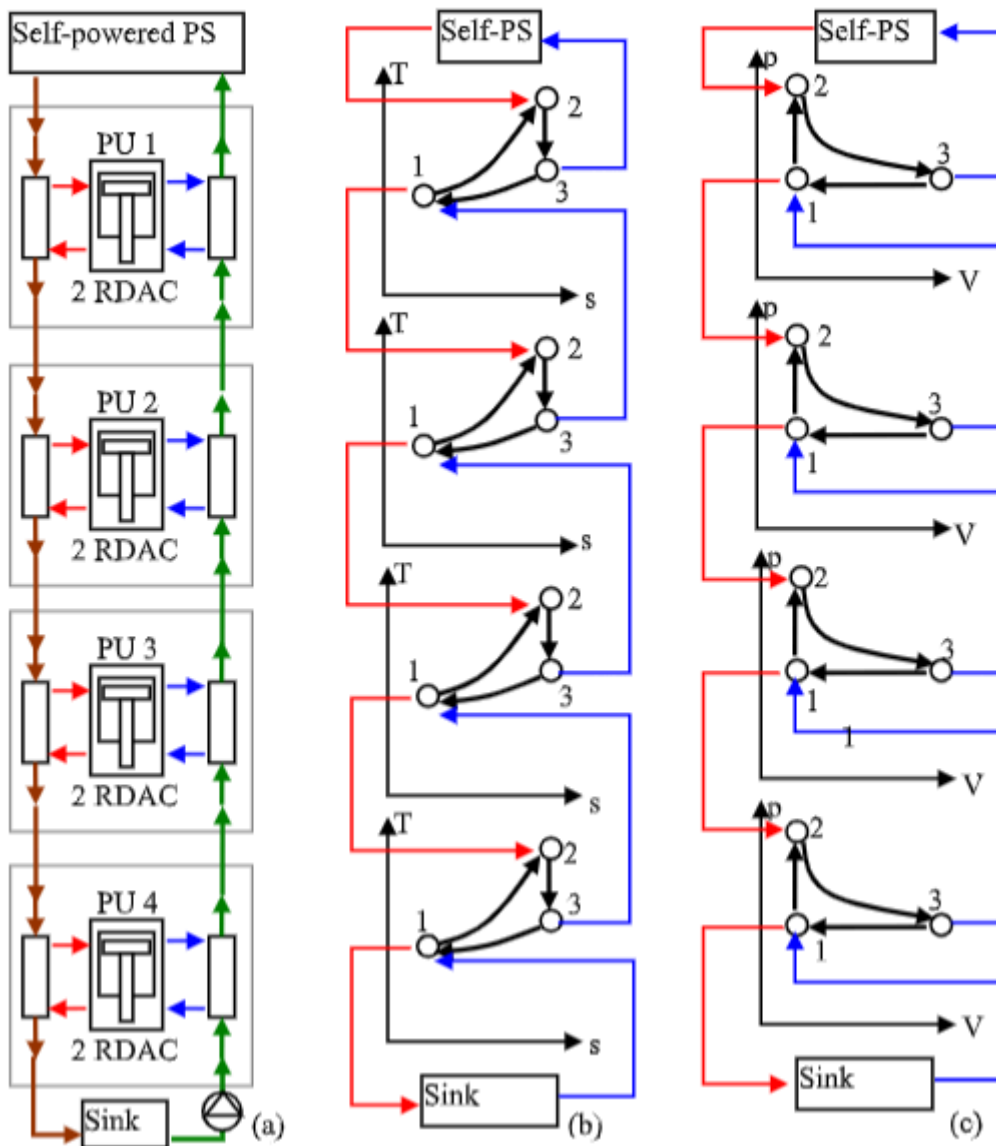


Figure 9: Heat energy supply flowchart of a self-powered power plant. The heat transfer closed circuit is responsible for adding and recovering heat to/from the cascaded power units depicted by V_{sp} thermal cycles by means of T-s and p-V diagrams coupled in cascade. (a): shows the symbolic structure of the HTF recirculation circuit. (b): shows the HTF recirculation circuit through the V_{sp} cycle represented by its T-s diagram. (c): shows the HTF recirculation circuit through the V_{sp} cycle represented by its p-V diagram.

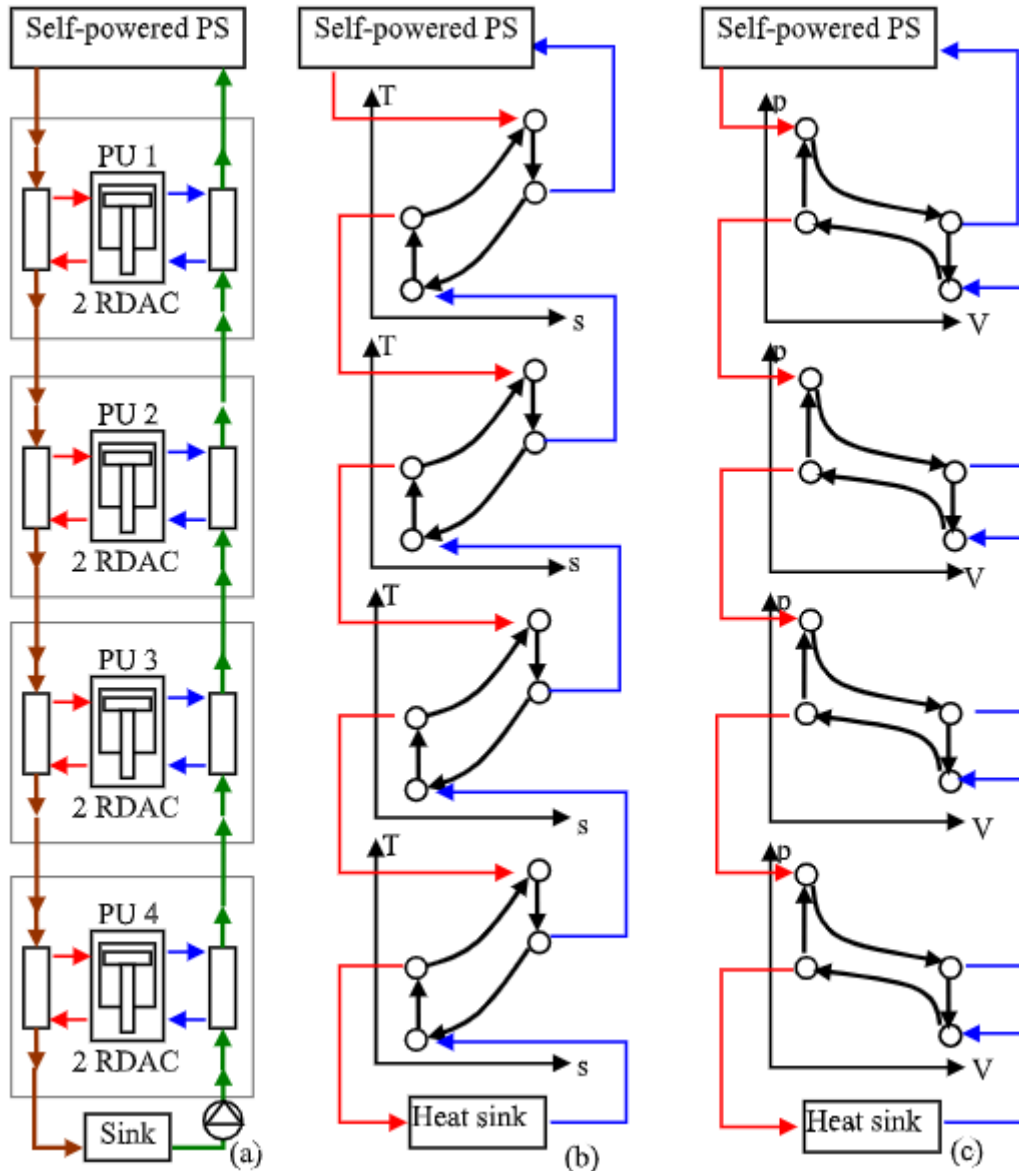


Figure 10: Heat energy supply flowchart of a self-powered power plant. The heat transfer closed circuit is responsible for adding and recovering heat to/from the cascaded power units depicted by VsVs thermal cycles by means of T-s and p-V diagrams coupled in cascade. (a): shows the symbolic structure of the HTF recirculation circuit. (b): shows the HTF recirculation circuit through the VsVs cycle represented by its T-s diagram. (c): shows the HTF recirculation circuit through the VsVs cycle represented by its p-V diagram.

4. Case studies

4.1 Achieving a self-sustaining energy strategy in adding and recovering heat

The basic scheme of a generic self-sustained thermal power plant equipped with the fundamental means to provide downstream heat to each PU coupled in cascade, as well as recover the cooling heat of each PU to be conducted upstream and feed back to the first PU (PU0) of the cascade, is represented in Figure 11. The useful mechanical work produced by each PU is converted to electrical power, being managed in such a way that a fraction of the electrical power is returned to the heat addition system to the PU0, while the remaining electrical power is sent to the network.

The fraction of electrical power sent to the PU0 is previously converted to heat by one of the available means: heating system based on electrical resistances, electro-inductive heating system or microwave heating system. Likewise, an alternative direct mechanical means of work-heat conversion through friction in a liquid could be used. The number of PUs in the plant is a function of two parameters: Temperature range available between the power source and the sink and the chosen value of the ratio (T_1/T_2), denoted as RIT for each PU.

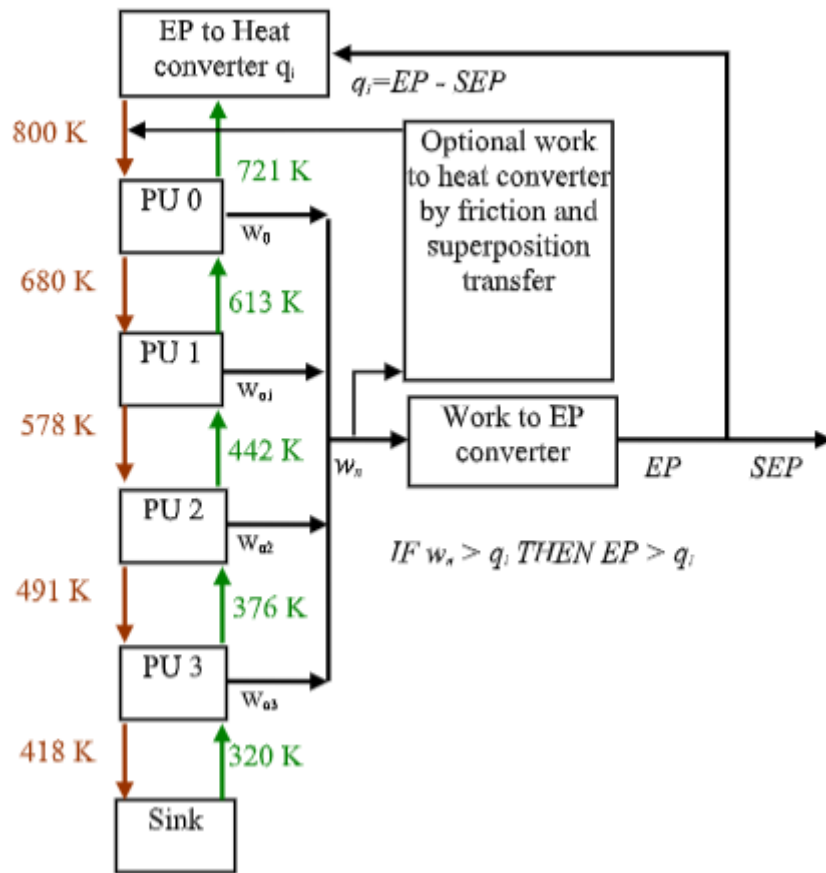


Figure 11: Schematic structure of a SPPP as the paradigm of a self sustaining power machine (SSPM) showing the inlet temperatures of every PU downstream with a RIT = 0.85, as well as the temperatures of the recovered heat of PUs upstream. Acronyms used are: EP, electrical power; SEP, self electrical power; EP-SEP, amount of heat to feed PU0.

According to the plant structure depicted in Figure 11, energy balance is carried out according to the following model:

The total mechanical work is defined as,

$$w_n = \sum_{i=1,n} w_i = w_o PU0 + w_o PU1 + w_o PU2 + w_o PU3 \tag{40}$$

where the required amount of heat to feed the first PU of the cascade structure, is given as

$$q_{i(PU1)} = EP - SEP \tag{41}$$

Thus, the condition to achieve a feasible SSPM is written as,

$$IF w_n > q_{i(PU1)} THEN SEP > 0 \tag{42}$$

This means that output electric power (EP) is greater than the added heat energy q_i , so that there exist a free-cost useful energy available, that is, SEP. Such condition is represented as

$$IF w_n > q_{i(PU1)} THEN EP > q_{i(PU1)} \tag{43}$$

So, starting from this notable difference in behaviour in terms of thermal efficiency between PUs that operate through expansion only (case of the Vsp thermal cycle) and PUs that operate through expansion and contraction (case of the VsVs thermal cycle), it is about analyzing both cases and draw the pertinent conclusions. The

structure of the analysis obeys the scheme shown in Figure 11 using equations (40-43) to compare the final results of each SSPM.

Energy management in each SSPM is carried out in accordance with the flow diagram of energy manipulated in heat-work-electrical energy interactions shown in Figure 12, such that the heat addition options can be electrical or mechanical: Among the electrical options we have heating techniques by electrical resistance, magnetic induction or microwave, while among the mechanical options we have friction in liquid fluids and drag in gaseous fluids.

Finally, the self-feeding index (SFI) is used to establish the quality criterion of the Self-feeding power plant (SFPP) in terms of the amount in percentage of nominal design power of energy obtained at free cost:

$$SFI(\%) = \frac{\eta_{th} - 100}{100} \quad (44)$$

According Equation (44), if the global thermal efficiency satisfies the condition ($\eta_{th} < 100$) then, SFI is negative, indicating the amount of heat tat required to have a perpetual motion machine of second kind.

4.2 Available heat scheduling schemes and adopted heating strategies

The task of adding heat to the first PU of the cascaded set of power units only can be implemented by means of devices capable for exhibiting heat superposition capacities. This means adding heat by increasing energy potential or temperature. This excludes de facto the heat transfer technique based on heat conduction via thermal fluids.

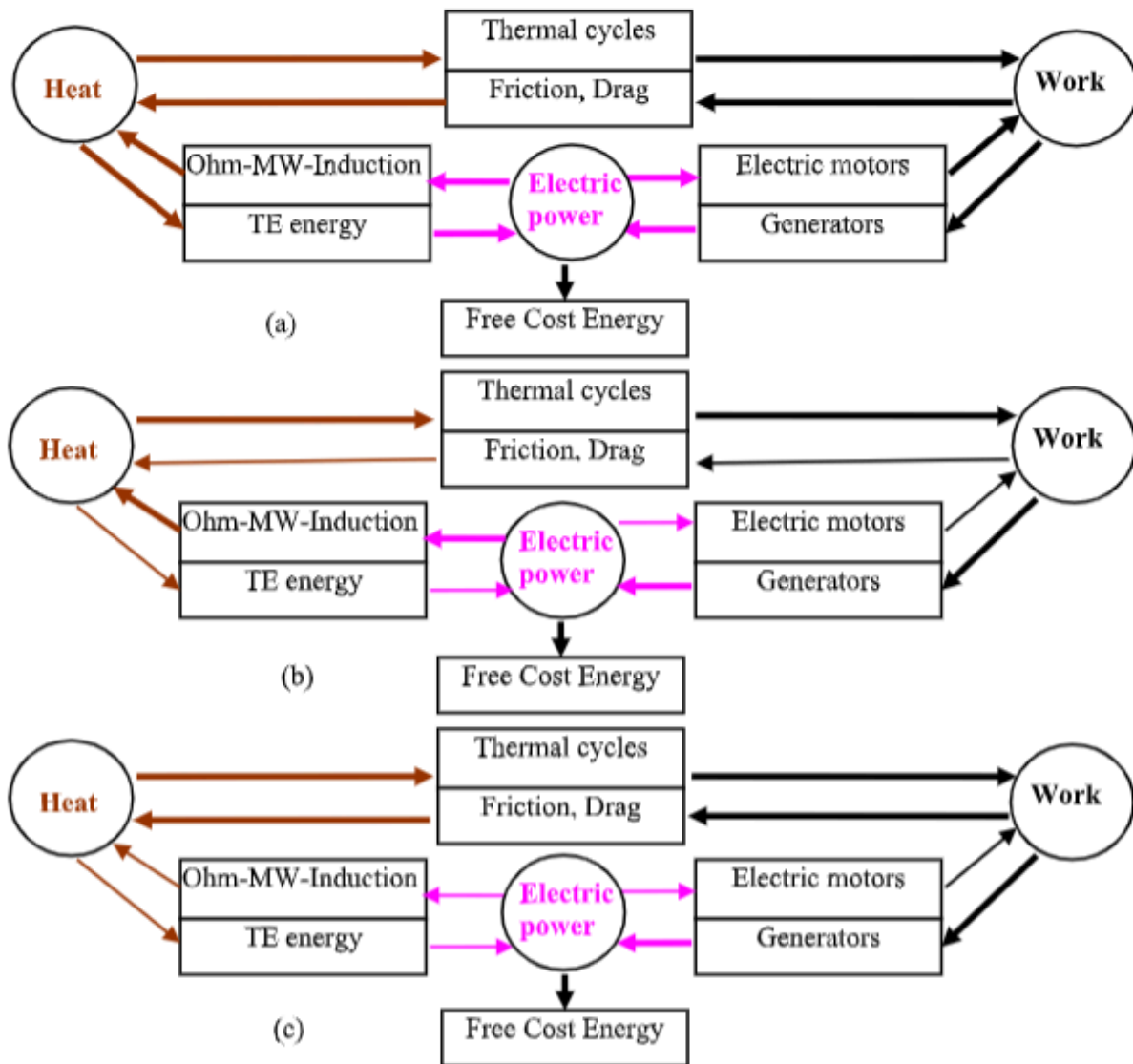


Figure 12: Common energy flow interactions in energy conversion tasks.

In Figure 12(a) it is shown the available optional interactions, while Figure 12(b) depicts the options based in adding heat by means by electric power- heat conversion using optionally: infrared heating by an electric resistance technique, micro-waves heating or magnetic induction heating. Finally Figure 12(c) illustrates the option based in adding heat by means of mechanical friction and/or drag (for the cases of liquid or gaseous fluids).

Well known techniques to transfer heat energy by superposition potential include mechanical and electrical devices. Among mechanical techniques there is friction and drag both exhibiting the property of converting the 100% of input added work to heat by friction. Thus in the Figure 12 it is depicted a scheme showing the applied option among the common energy flow interactions in energy conversion tasks. While in (a) it is shown the available optional interactions, in (b) it is shown the option based in adding heat by means of electric power-heat conversion using optionally: electric-resistance heating, micro-waves heating or magnetic induction heating, and finally in (c) it is shown the option based in adding heat by means of mechanical friction and/or drag (for the cases of liquid or gaseous fluids).

4.3 Case study 1: SSPM based on cascaded PUs equipped with the Vsp cycle for air and helium as working fluids

The study to be carried out in case 1 studies a variety of thermal cycles characterized by closed processes that perform mechanical work only through the expansion of the thermal working fluid denoted as Vps. Traditionally, it is characterized by obeying the Clausius and Kelvin-Planck statement since the heat supplied is equivalent to the sum of the work obtained and the heat evacuated to a thermal sink. That is, it is a conventional thermal cycle,

which, as has been demonstrated in section 2.5 and Figure 2, exceeds the Carnot factor under certain operating conditions.

The Vsp thermal cycle that has been depicted in Figure 1(b) and (c), lacks thermal contraction and therefore only performs useful mechanical work by expanding the thermal working fluid. In this study, both individual and collective thermal efficiency is tested, that is, when it constitutes a thermal power plant formed by a group of VsVs thermal cycles coupled in cascade in such a way that the cascade coupling structure composed by PUs ends when the heat exhausted by the last downstream cycle at its lowest temperature reaches a working temperature incapable to produce useful work. Likewise, the heat rejected by each Vsp thermal cycle is recovered upstream so that it can be reused through feedback to the first cycle of the cascade.

The resulting thermal power plant is shown in Figure 13, in which Figure 13 (a) operates with air as the thermal working fluid, while Figure 13 (b) operates with helium as the thermal working fluid. In this study, the results of both thermal work fluids are compared, where it is observed that air is still valid to produce more mechanical work than the heat demanded to function as a self-sustained plant, providing a valid SFI value with a RIT of 0.85. Similarly, when operating with helium, significantly higher results are obtained in terms of the SFI value for a RIT of 0.85.

The data resulting from processing the Vsp cycle states for air and helium at each PU are shown in Table 6 using air and helium as a real working fluids (Lemmon E.W. et al., 2007) [24].

Table 6 Vsp cycles data for air and helium as working fluids with RIT = 0.85 for the seven PUs of each power plant case study.

SPs	T(K)	p(bar)	v(m ³ /kg)	u(kj/kg)	s(kj/kg.K)	T(K)	p(bar)	v(m ³ /kg)	u(kj/kg)	s(kj/kg.K)
PU0-Air						PU0-Helium				
1	680	1	0.97048	623.08	4.531	680	1	7.01880	2124.00	30.804
2	800.00	1.3553	0.97048	718.79	4.661	800.00	1.3553	7.01880	2497.90	31.310
3	766.60	1	1.09410	691.82	4.661	749.65	1	7.73740	2341.00	31.310
PU1						PU1-Helium				
1	614.81	1	0.87744	572.52	4.424	607.60	1	6.27190	1898.40	30.219
2	723.30	1.3556	0.87744	657.20	4.551	714.83	1.3553	6.27190	2232.50	30.725
3	692.59	1	0.98844	632.96	4.551	669.78	1	6.91340	2092.10	30.725
PU2-Air						PU2-Helium				
1	555.64	1	0.79298	527.49	4.318	542.89	1	5.60420	1696.70	29.634
2	653.70	1.3557	0.79298	602.54	4.442	638.69	1.3552	5.60420	1995.30	30.141
3	625.53	1	0.89275	580.77	4.442	598.54	1	6.17840	1870.10	30.141
PU3-Air						PU3-Helium				
1	502.00	1	0.71639	487.32	4.213	485.11	1	5.00810	1516.70	29.050
2	590.59	1.3558	0.71639	553.97	4.335	570.71	1.3552	5.00810	1783.40	29.556
3	564.80	1	0.80606	534.41	4.335	534.78	1	5.52050	1671.40	29.556
PU4-Air						PU4-Helium				
1	453.39	1	0.64696	451.40	4.108	433.45	1	4.47510	1355.70	28.465
2	533.40	1.3559	0.64696	510.73	4.229	509.94	1.3553	4.47510	1594.10	28.972
3	509.82	1	0.72756	493.14	4.229	477.89	1	4.93370	1494.20	28.972
PU5-Air						PU5-Helium				
1	409.36	1	0.58404	419.19	4.004	387.32	1	3.99920	1212.00	27.881
2	481.60	1.3553	0.58404	472.16	4.123	455.67	1.3553	3.99920	1425.00	28.387
3	460.09	1	0.65652	456.32	4.123	426.98	1	4.40840	1335.60	28.387
PU6-Air						PU6-Helium				

1	369.52	1	0.52708	390.25	3.900	346.08	1	3.57370	1083.50	27.296
2	434.73	1.3563	0.52708	437.67	4.018	407.15	1.3553	3.57370	1273.80	27.802
3	415.17	1	0.59234	423.42	4.018	381.49	1	3.93910	1193.80	27.802

In Figure 13, the cascaded structure of the seven Power Units (PUs) in each Self-Sustained Power Module (SSPM) is depicted. The SSPM shown in Figure 13(a) operates with **air** as the working fluid, while the SSPM depicted in Figure 13(b) uses **helium** as the working fluid. For each PU within the cascaded SSPM of Figure 13, the temperatures of the input-added and recovered heats to/from any PU are shown. Notably, some heat is released to the heat sink from the last PU downward. However, a significant portion of this heat could potentially be recovered and utilized by another cascaded PU that is not explicitly represented.

Table 7 presents data resulting from the Vsp thermal cycle analysis for both air and helium as working fluids. The structure of Table 7 aligns with the first column, where LF/PU_i , RF/PU_i , $RIT*100/PU_i$, T_2/PU_i [K], and T_1/PU_i [K] represent input variables. Additionally, the output variables— q_{in2}/PU_i [kJ/kg], q_{o34}/PU_i [kJ/kg], q_{rec}/PU_i [kJ/kg], T_{q-rec}/PU_i [K], w_n/PU_i [kJ/kg], η_{th}/PU_i [%], $\eta_{th}/plant$ [%], and $SFI\%/plant$ —are assumed as results.

These results in Table 7 serve as a guide for designing prototypes and establishing useful design criteria. Furthermore, they allow us to assess the validity of the proposed input data based on the output results that best align with the expected performance of the implemented prototype. The energy balance, based on the first law and described by Equations (1)–(6), has been considered in this study.

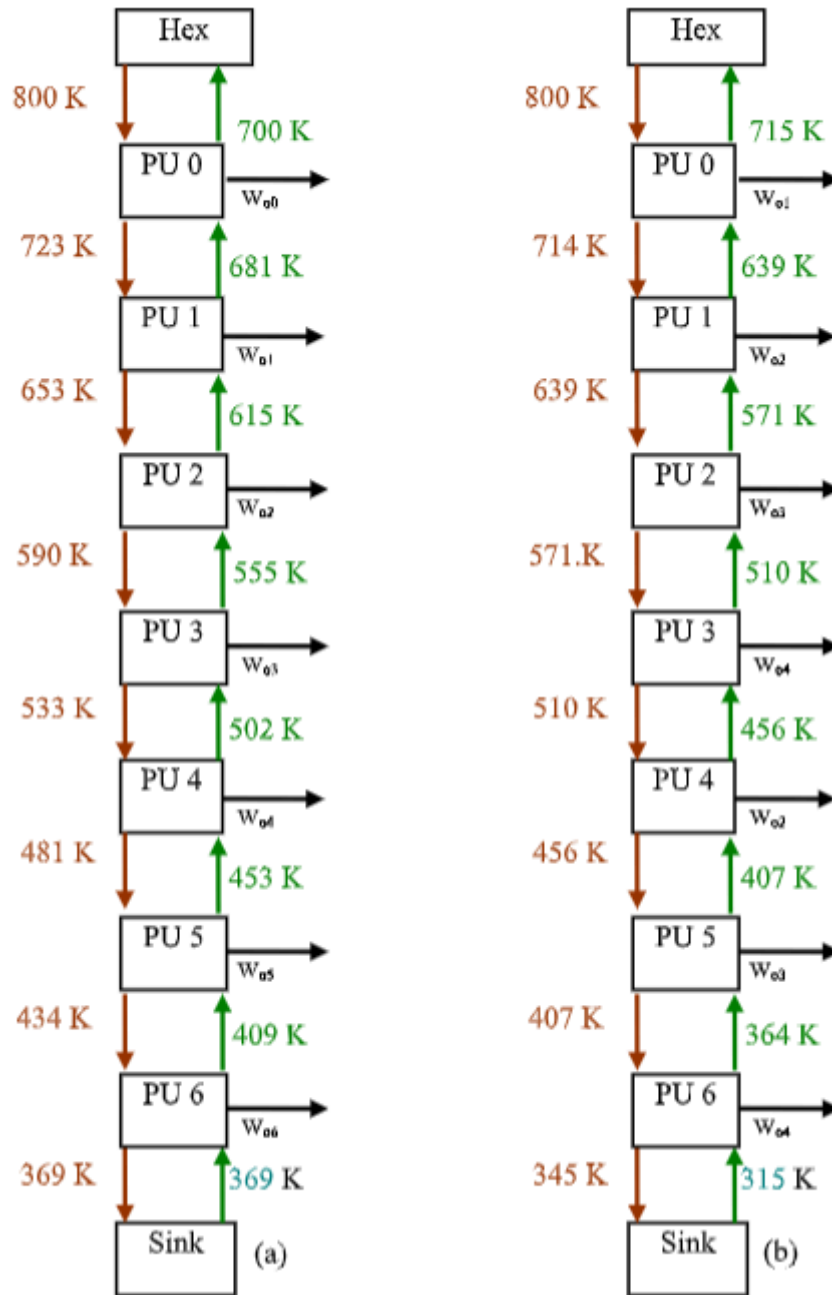


Figure 13: Case studies 1 based on a Vsp cycle: (a) SSPM operating with air as working fluid, showing the temperatures of the adding heat to any PU. (b) SSPM operating with He as working fluid, showing the temperatures of the input added and recovered heats to/from any PU.

Table 7 Results of case studies with the data from Table 6 for the irreversible SSPM composed of seven cascaded PUs operating with air and helium as working fluids under Vsp cycles implemented under the structures depicted in Figures 13(a) and 13(b).

Results of case studies of the cycle Vsp with air as working fluid								
PU _i	0	1	2	3	4	5	6	total
LF/PU _i	0.9	0.9	0.9	0.9	0.9	0.9	0.9	
RF/PU _i	0.85	0.85	0.85	0.85	0.85	0.85	0.9	
RIT*100/PU _i	85.0	85.0	85.0	85.0	85.0	85.0	85.0	
T ₂ /PU _i [K]	800.00	723.30	653.70	590.59	533.40	481.60	434.73	

T_1/PUi [K]	680	614.81	555.64	502.00	453.39	409.36	369.52	
q_{in2}/PUi [kJ/kg]	95.71	84.68	75.05	66.65	59.33	52.97	47.42	481.81
q_{o34}/PUi [kJ/kg]	68.74	60.44	53.28	47.09	41.74	37.13	33.17	
q_{rec}/PUi [kJ/kg]	58.43	51.37	45.29	40.03	35.48	31.56	29.85	292.10
T_{q-rec}/PUi [K]	723.30	653.70	590.59	533.40	481.60	434.73	392.34	
w_n/PUi [kJ/kg]	20.63	18.54	16.65	14.96	13.46	12.12	11.54	107.91
η_{th}/PUi [%]	21.56	21.90	22.19	22.45	22.68	22.88	24.34	22
$\eta_{th}/plant$ [%]								56.85
SFI %/PP								-43.15

Results of case studies of the cycle Vsp with helium as working fluid

PUi	0	1	2	3	4	5	6	total
LF/PUi	0.9	0.9	0.9	0.9	0.9	0.9	0.9	
RF/PUi	0.85	0.85	0.85	0.85	0.85	0.85	0.85	
RIT*100/PUi	85.0	85.0	85.0	85.0	85.0	85.0	85.0	
T_2/PUi [K]	800.00	714.83	638.69	570.71	509.94	455.67	407.15	
T_1/PUi [K]	680	607.60	542.89	485.11	433.45	387.32	346.08	
q_{in2}/PUi [kJ/kg]	373.90	334.10	298.60	266.70	238.40	213.00	190.30	1915.90
q_{o34}/PUi [kJ/kg]	217.00	193.70	173.40	154.70	138.50	123.60	110.30	
q_{rec}/PUi [kJ/kg]	184.45	164.65	147.39	131.50	117.73	105.06	93.76	944.52
T_{q-rec}/PUi [K]	714.83	638.69	570.71	509.94	455.67	407.15	363.78	
w_n/PUi [kJ/kg]	120.03	107.41	95.78	85.68	76.42	68.39	61.20	614.91
η_{th}/PUi [%]	32.10	32.15	32.08	32.13	32.06	32.11	32.16	32
$\eta_{th}/plant$ [%]								63.36
SFI %/PP								-36.64

The case study results, obtained from the data in Table 6, pertain to an irreversible SSPM composed of seven cascaded PUs operating with air and helium as working fluids under Vsp cycles. These results focus on the SSPM’s performance, particularly the SFI (Self-Sufficiency Index), as a function of the RIT (Recovered Input Temperature) considered to be 0.85. The assumptions include a heat recovery factor (RF) of 0.85 and a losses factor (LF) of 0.9.

4.4 Case study 2: SSPM based on cascaded PUs equipped with the VsVs cycle for air and helium as working fluids

The study to be carried out in case 2 denoted as VsVs studies a variety of thermal cycles characterized by closed processes that perform mechanical work both through the expansion and contraction of the thermal working fluid. This cycle is not traditional, being characterized by violating the balance of energy (heat and work) associated with the heat-work interactions.

The VsVs thermal cycle shown in Figure 4 (b) and (c) exhibit thermal contraction and therefore performs useful mechanical work by expanding and contracting the thermal working fluid. In this study, both individual and collective thermal efficiency is tested, that is, when it constitutes a thermal power plant formed by a group of VsVs thermal cycles coupled in cascade in such a way that the cascade coupling structure composed by PUs ends when the heat exhausted by the last downstream cycle at its lowest temperature reaches a working temperature incapable to produce useful work. Likewise, the heat rejected by cooling each VsVs thermal cycle is recovered upstream so that it can be reused through feedback to the first cycle of the cascade.

The resulting thermal plant is shown in Figure 14, in which Figure 14 (a) operates with air as the thermal working fluid, while Figure 14 (b) operates with helium as the thermal working fluid. In this study, the results of both thermal work fluids are compared, where it is observed that air is still valid to produce more mechanical work than the heat demanded to function as a self-sustained plant, providing a valid SFI value with a RIT of 0.85.

Similarly, when operating with helium, significantly higher results are obtained in terms of the SFI value for a RIT of 0.85.

The data resulting from processing the VsVs cycle states for air and helium at each PU are shown in Table 8 using real gas values obtained from the NIST database.

Table 8 VsVs cycle data for air and helium as working fluids with RIT = 0.85

SPs	T(K)	p(bar)	v(m ³ /kg)	u(kJ/kg)	s(kJ/kg.K)	T(K)	p(bar)	v(m ³ /kg)	u(kJ/kg)	s(kJ/kg.K)
PU0-Air					PU0-Helium					
1	680.0 0	1	0.97048	623.08	4.531	680.0 0	1	7.01880	2124.00	30.804
2	800.0 0	1.3555	0.97048	718.79	4.661	800.0 0	1.3553	7.01880	2497.90	31.310
3	766.6 0	1	1.09410	691.82	4.661	749.65	1	7.73740	2341.00	31.310
4	650.7	0.6954	1.09410	600.25	4.531	637	0.6975	7.73740	1990.00	30.804
PU1-Air					PU1-Helium					
1	578.0 0	1	0.82490	544.41	4.359	578.0 0	1	5.96650	1806.10	29.960
2	680.0 0	1.3556	0.82490	623.06	4.484	680.0 0	1.3552	5.96650	2124.00	30.466
3	650.8 6	1	0.92890	600.36	4.484	637.20	1	6.57720	1990.60	30.466
4	552.5 0	0.6955	0.92890	525.15	4.359	542.0 0	0.6992	6.57720	1693.90	29.960
PU2-Air					PU2-Helium					
1	491.30	1	0.7011	479.38	4.1906	491.30	1	5.0720	1536.00	29.116
2	578.0 0	1.3558	0.7011	544.39	4.3124	578.0 0	1.3552	5.0720	1806.20	29.622
3	552.69	1	0.7888	525.26	4.3124	541.62	1	5.5911	1692.80	29.622
4	469.3 0	0.6958	0.7888	463.14	4.1906	460.6 0	0.6989	5.5911	1440.30	29.116
PU3-Air					PU3-Helium					
1	417.61	1	0.59583	425.20	4.024	417.61	1	4.31170	1306.40	28.272
2	491.30	1.3560	0.59583	479.34	4.144	491.30	1.3552	4.31170	1536.00	28.778
3	469.39	1	0.66981	463.17	4.144	460.37	1	4.75290	1439.60	28.778
4	398.7 0	0.6963	0.66981	411.47	4.024	391.50	0.6988	4.75290	1225.00	28.272
PU4-Air					PU4-Helium					
1	354.96	1	0.50626	379.72	3.860	354.96	1	3.66540	1111.10	27.428
2	417.61	1.3564	0.50626	425.16	3.978	417.61	1.3553	3.66540	1306.40	27.934
3	398.78	1	0.56893	411.49	3.978	391.31	1	4.04040	1224.40	27.934
4	338.7 0	0.69591	0.56893	368.03	3.860	332.70	0.6984 8	4.04040	1041.80	27.428

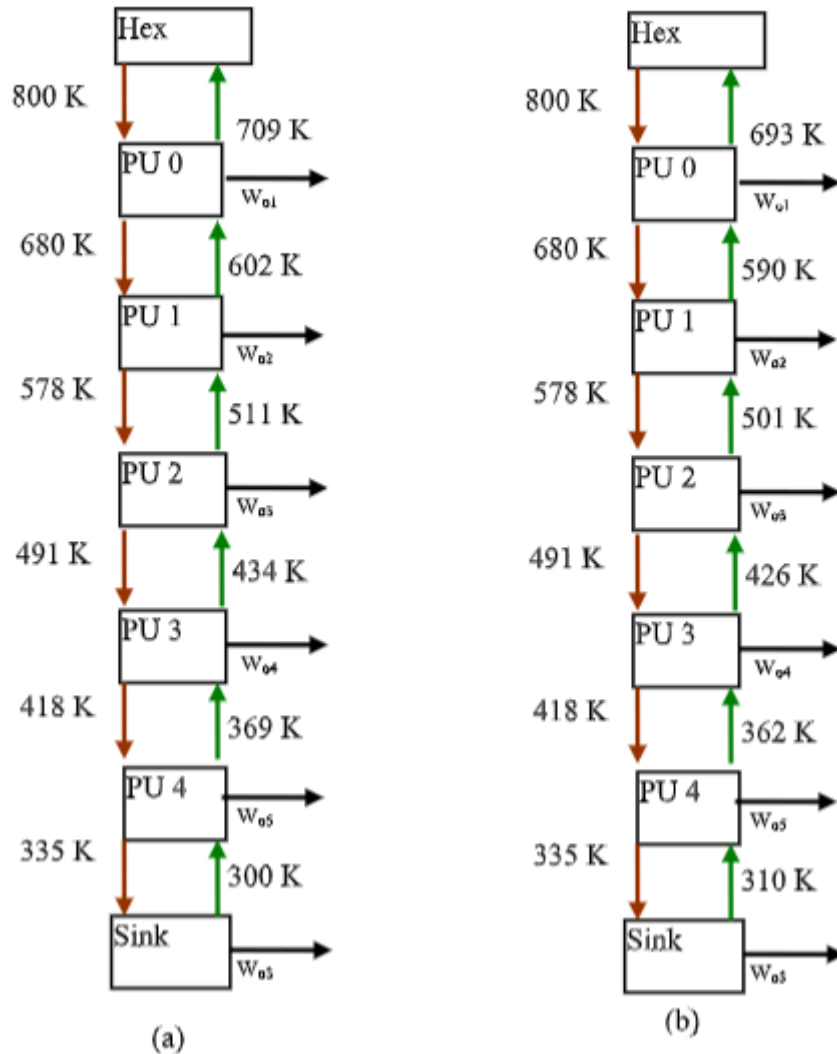


Figure 14: Case studies 1 based on a VsVs cycle: (a) SSPM operating with air as working fluid. (b) SSPM operating with helium as working fluid

In Figure 14, the cascaded structure of the seven Power Units (PUs) in each Self-Sustained Power Module (SSPM) is depicted. The SSPM shown in Figure 14(a) operates with **air** as the working fluid, while the SSPM depicted in Figure 14(b) uses **helium** as the working fluid. For each PU within the cascaded SSPM of Figure 14, the temperatures of the input-added and recovered heats to/from any PU are shown. Notably, some heat is released to the heat sink from the last PU downward. However, a significant portion of this heat could potentially be recovered and utilized by another cascaded PU that is not explicitly represented.

Table 8 presents data resulting from the VsVs thermal cycle analysis for both air and helium as working fluids. The structure of Table 8 aligns with the first column, where LF/PU_i, RF/PU_i, RIT*100/PU_i, T₂/PU_i [K], T₁/PU_i [K] represent input variables. Additionally, the output variables—q_{in2}/PU_i [kJ/kg], q_{o34}/PU_i [kJ/kg], q_{rec}/PU_i [kJ/kg], T_{q-rec}/PU_i [K], w_n/PU_i [kJ/kg], η_{th}/PU_i [%], η_{th}/plant [%], and SFI %/plant—are assumed as results.

These results in Table 9 are in concordance with those of Table 7 having into account the differences inherent to the characteristics of both cycles and serve also as a guide for designing prototypes and establishing useful design criteria. Furthermore, they allow us to assess the validity of the proposed input data based on the output results that best align with the expected performance of the implemented prototype. The energy balance, based on the first law and described by Equations (8)–(13), has been considered in this study.

Table 9 Results of case studies with the data from Table 8 for the irreversible SSPM composed of five cascaded PUs operating with air as a working fluid under VsVs cycles obeying to the scheme depicted in Figure 14(a) and with helium as a working fluid under VsVs cycles obeying to the scheme depicted in Figure 14(b)

Results of case studies of the cycle VsVs with air as working fluid

PUi	0	1	2	3	4	total
LF/PUi	0.9	0.9	0.9	0.9	0.9	
RF/PUi	0.85	0.85	0.85	0.85	0.85	
RIT*100/PUi	85.0	85.0	85.0	85.0	85.00	
T ₂ /PUi [K]	800.00	680.00	578.00	491.30	417.61	
T ₁ /PUi [K]	680.00	578.00	491.30	417.61	354.96	
q _{in2} /PUi [kJ/kg]	95.71	78.65	65.01	54.14	45.44	338.95
q _{o34} /PUi[kj/kg]	91.57	75.21	62.12	51.70	43.46	
q _{rec} /PUi[kj/kg]	77.83	63.93	52.80	43.95	36.94	234.13
T _{q-rec} /PUi [K]	708.65	601.68	511.00	434.05	368.74	
w _n /PUi[kj/kg]	38.10	32.10	27.06	22.87	19.40	139.53
η _{th} /PUi [%]	39.80	40.81	41.62	42.25	42.69	41
η _{th} /plant [%]						113.15
SFI %/PP						33.12

Results of case studies of the cycle VsVs with helium as working fluid

PU	0	1	2	3	4	total
LF/PUi	0.9	0.9	0.9	0.9	0.9	
RF/PUi	0.85	0.85	0.85	0.85	0.85	
RIT*100/PUi	85.0	85.0	85.0	85.0	85.00	
T ₂ /PUi [K]	800.00	680.00	578.00	491.30	417.61	
T ₁ /PUi [K]	680.00	578.00	491.30	417.61	354.96	
q _{in2} /PUi [kJ/kg]	373.90	317.90	270.20	229.60	195.30	1386.90
q _{o34} /PUi[kj/kg]	351.00	296.70	252.50	214.60	182.60	
q _{rec} /PUi[kj/kg]	298.35	252.20	214.63	182.41	155.21	937,37
T _{q-rec} /PUi [K]	693.33	589.60	501.11	425.94	362.01	
w _n /PUi[kj/kg]	222.54	187.88	159.96	136.02	115.74	822.15
η _{th} /PUi [%]	59.52	59.10	59.20	59.24	59.26	59
η _{th} /plant [%]						182.89
SFI %/PP						82.89

The case study results, obtained from the data in Table 8, pertain to an irreversible SSPM composed of seven cascaded PUs operating with air and helium as working fluids under Vsp cycles. These results focus on the SSPM's performance, particularly the SFI (Self-Sufficiency Index), as a function of the RIT (Recovered Input Temperature) considered to be 0.85. The assumptions include a heat recovery factor (RF) of 0.85 and a losses factor (LF) of 0.9.

5 Analysis of results

Figures 15 to 18 illustrate the behavior of each thermal cycle in terms of the heat added to the cycle, the useful work obtained, and the associated thermal efficiency. The results for the Vsp cycle, operating with both air and helium, are depicted in Figures 15 and 16. Similarly, the results for the VsVs cycle, also operating with air and helium, are presented in Figures 17 and 18.

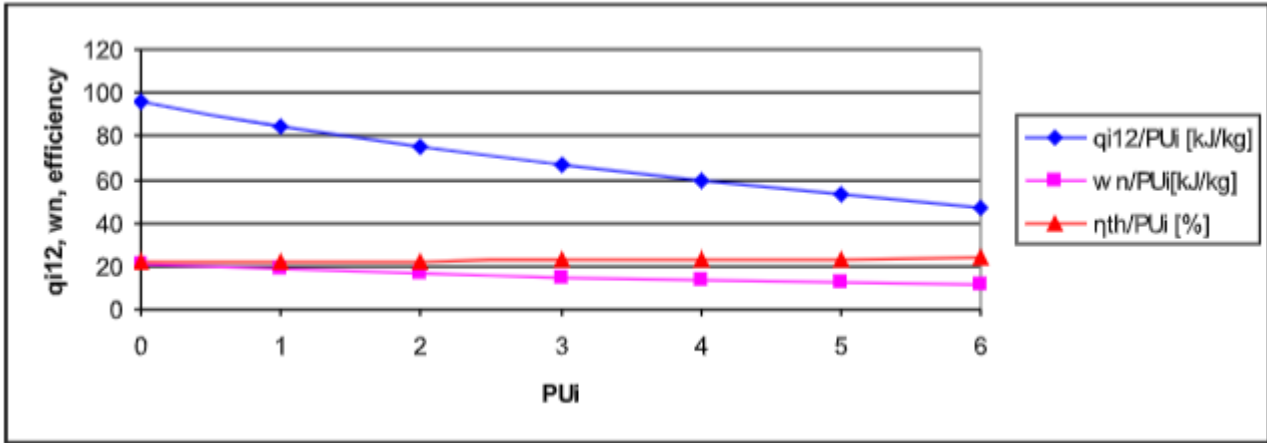


Figure 15: Added heat q_{i12} , net useful work w_n , and thermal efficiency η_{th} of each PU (0-6) operating with air as working fluid under a Vsp thermal cycle with data retrieved from Table 7

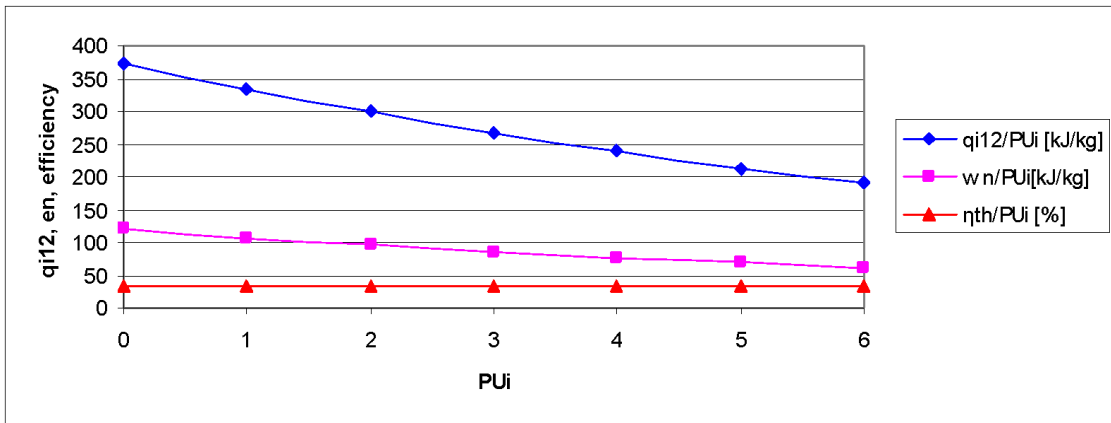


Figure 16: Added heat q_{i12} , net useful work w_n , and thermal efficiency η_{th} of each PU (0-6) operating with helium as working fluid under a Vsp thermal cycle with data retrieved from Table 7.

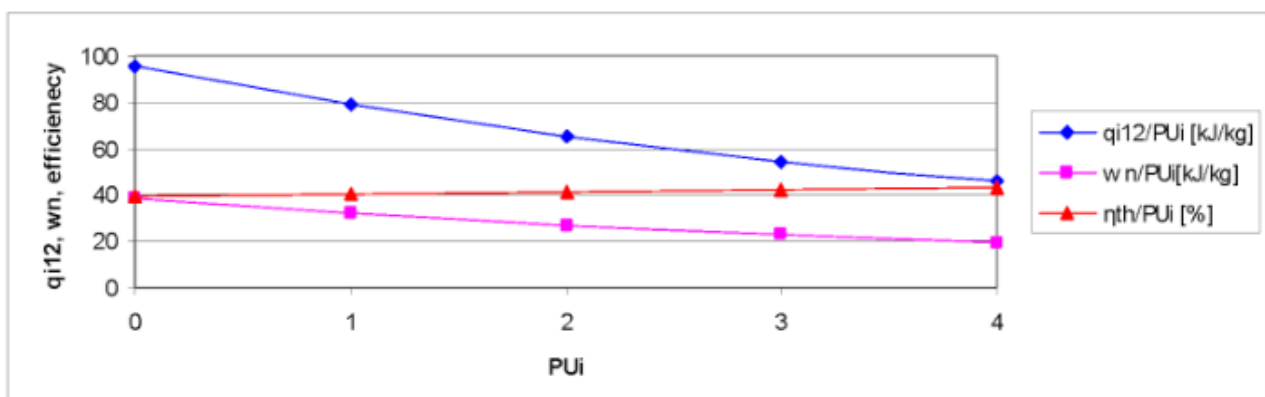


Figure 17: Added heat q_{i12} , net useful work w_n , and thermal efficiency η_{th} of each PU (0-4) operating with air as working fluid under a VsVs thermal cycle with data retrieved from Table 9.

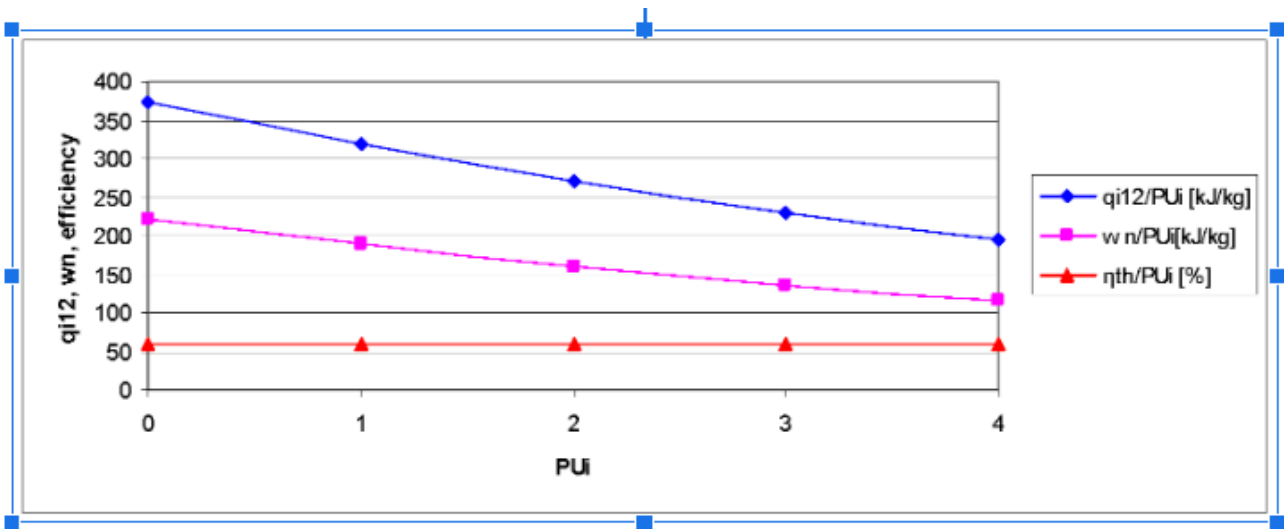


Figure 18: Added heat q_{i12} , net useful work w_n , and thermal efficiency η_{th} of each PU (PU0 to PU4) operating with helium as working fluid under a VsVs thermal cycle with data retrieved from Table 9.

It is noteworthy that the thermal efficiencies among the Vsp cycles remain nearly constant as the peak temperatures decrease, even when the thermal fluids are considered as real gases. This constancy is attributed to the temperature ratios (RIT = T_1/T_2) within each cycle adhering to the preselected value for the RIT, which is optionally chosen to be constant; in these case studies, the value is 0.85. A similar observation applies to the VsVs thermal cycle: the thermal efficiencies are not influenced by the peak temperatures but rather by the temperature ratios. Even with thermal fluids treated as real gases, the efficiencies remain almost constant.

Table 10 Global data resulting from tables 7 and 9 derived from case studies 1 and 2 respectively.

	Vsp cycle (case study 1 table 7)		VsVs cycle (case study 2 table 9)	
Number of PUs	7		5	
Thermal fluid	Air	Helium	Air	Helium
q_{i12}/PU_i [kJ/kg]	95.71	373.90	338,95	1386,90
w_n/PU_i [kJ/kg]	107.91	614.91	139,53	822,15
$\eta_{th}/plant$ [%]	56.85	63.36	133,12	182,89
SFI [%]/plant	-43.15	-36.64	33,12	82,89

Table 10 presents the comprehensive results for the two power plant cases studied, equipped with Vsp and VsVs thermal cycles, respectively. In both scenarios, the thermal working fluids—air and helium—have been treated as real gases.

The most significant aspect of the global results for the thermal power plants utilizing Vsp and VsVs cycles, as shown in Table 10, is the SFI (Self-Feed Index) value, which is defined in Section 4.1. For a thermal plant equipped with 7 Power Units (PUs) and using air as the thermal working fluid, the SFI value is **-43.15**, corresponding to an efficiency of **56.85%**. In contrast, a thermal power plant with 7 PUs using helium as the thermal working fluid yields an SFI value of **-36.64**, equating to an efficiency of **63.36%**.

Similarly, a thermal power plant with 5 PUs operating with air as the thermal working fluid delivers an SFI value of **33,12**, which translates to an efficiency of **133.12%**. Meanwhile, a thermal plant with 5 PUs and using helium as the thermal working fluid achieves an SFI value of **82.88**, equivalent to an efficiency of **182.89%**.

Consequently, based on the case studies object of the researched topic carried out in this section, which are focused on the fact that each Power Unit (PU), whose thermal cycle produces useful mechanical work through the thermal contraction of the TWF for VsVs thermal cycles, nearly doubles the useful work output compared to conventional thermodynamic cycles (which operate solely through the expansion of the TWF such that the Vsp cycles).

As a result, a series of thermal cycles functioning through contraction can potentially double the total useful work output in comparison to traditional thermal cycles.

Notwithstanding this notable result, it is also observable in the case of applying the same heat recovery system to plants formed by cascades of PUs that operate exclusively with the Vsp thermal cycle, which lacks the ability to produce work by thermal contraction of the working fluid.

Furthermore, if we consider the added benefit of recuperating the heat expended for cooling—which is responsible for the thermal contraction in each PU—and if this recovered heat is reintegrated into the power supply, it becomes apparent that the system can generate more useful work than the heat input required to power the first PU in the cascaded structure of PUs.

The overall results obtained with respect to the overall thermal efficiency shown in Tables 7 and 9 appear to represent a flagrant violation of the principle of energy conservation. However, all the Power Units (PUs) used in the implementation of the thermoelectric plants in both cases studied exhibit thermal efficiencies with values notably lower than 100% of the ideally possible efficiency.

Given the current scenario, how is it possible that with a group of PUs coupled in cascade, whose individual thermal efficiencies are much less than 100%, a global amount of useful work greater than the amount of heat required to power the single PU that needs external heat to ensure the operation of the thermoelectric power plant without additional heat requirements. According to the average values of the thermal efficiency corresponding to the individual PUs that forms a SSPP observed in Tables 7 and 9, we have:

Vsp cycle with air:	22%
Vsp cycle with helium:	32%
VsVs cycle with air:	41%
VsVs cycle with helium:	59%

From the above data, the following facts are deduced:

- The global efficiencies of the SSPP equipped with PUs operating with Vsp cycles is about the 50% of the efficiencies achieved with PUs operating with VsVs cycles, and,
- The global efficiencies of the SSPP equipped with PUs operating with air as working fluid is about 33% less than the SSPP equipped with PUs operating with helium as working fluid.

Therefore, the achievement of overall thermal efficiencies that exceed the ideally possible 100% limit value is exclusively due to the upstream cascade heat recovery strategy. The heat recovered in conventional power engines consists mainly in low-grade heat, so that the opportunities to be efficiently reused as complement to the main power has been lost. However, as seen, previously in this work it is observed that the heat recovered has been upgraded by increasing its temperature or heat potential so that heat can be transferred to be efficiently reused. Such method concerns to infrared-based electric heating technique by resistance heating or direct radiation, or by induction-based heating or by microwave radiation-based heating.

4. Conclusions

The presented article, “Prototyping a Disruptive Self-Sustaining Power Plant enabled to overcome a Perpetual Motion Machine”, presents a methodology to implement a self-sustaining power plant (SSPP) that defies conventional laws of thermodynamics.

To achieve such a level of improvements, some disruptive contributions have been carried out that gave rise to the following controversies with respect to the conventional statements:

- Carnot factor is systematically defied, so that needs a redefinition to operate only between two isothermal temperatures
- Exergy concept needs revision due to the additional contraction-based work,
- First law needs revision:
 - 1-the energy balance of thermal cycles with contraction-based work needs revision and
 - 2- the energy balance of any SSPP needs revision.
- Second law needs revision since it is impossible a device operating on a cycle that:

Clausius statement: transfer heat from a cooler body to a hotter body **without external work**

Kelvin-Planck statement: produce work and transfer heat from a single body **without a heat sink**

As consequence, based on the method and clarity of the rigorous reasoning presented throughout the article, we are convinced that the contributions made are responsible for the controversy raised. This leads us to take precautions regarding the confidence we place in the results that lack experimental validation.

Thus, since the research proposes a system in which the heat released by each power unit (PU) is efficiently recovered and reused, which could result in efficiency exceeding 100% under certain conditions, this would suggest a violation of the principle of conservation of energy and the possibility of overcoming a perpetual motion machine of the second type.

However, we are aware that it is important to recognise and note that, according to the fundamental laws of physics, perpetual motion machines are impossible. The first law of thermodynamics states that energy cannot be created or destroyed, it can only be transformed. The second law indicates that the entropy of an isolated system tends to increase, as consequence of irreversibilities including energy losses in the form of non-recoverable heat. As consequence, we are sure that the results presented in the article should be interpreted with caution. Although the idea of a power plant that can operate at greater than 100% efficiency is intriguing, it contradicts current understanding of the laws of thermodynamics. Since the article explores some theoretical and/or hypothetical concepts that have not yet been practically demonstrated, further effort must be done to remove any doubt, about the need for experimental validation. Consequently, based on the controversy raised by the results of both the positive proofs of concept on double-acting cylinders operating by expansion and vacuum or contraction as well as the empirical calculations with real gases assuming irreversibilities, there is only one irrefutable method to settle the discussion: validation through experimental tests on a significant prototype.

References

1. Wikipedia. Thomas Savery. https://en.wikipedia.org/wiki/Thomas_Savery.
2. Wikipedia. Thomas Newcomen. https://en.wikipedia.org/wiki/Thomas_Newcomen.
3. Wikipedia. James Watt: https://en.wikipedia.org/wiki/James_Watt. and https://en.wikipedia.org/wiki/Watt_steam_engine.
4. Müller. Gerald. The atmospheric steam engine as energy converter for low and medium temperature thermal energy. *Renewable energy*. 2013. vol. 53. p. 94-100. <https://doi.org/10.1016/j.renene.2012.10.056>;
5. Gerald Müller. George Parker. Experimental investigation of the atmospheric steam engine with forced expansion. *Renewable Energy*. Vol. 75. 2015. pp 348-355. ISSN 0960-1481. <https://doi.org/10.1016/j.renene.2014.09.061>.
6. Vitor Augusto Andreghetto Bortolin. Bernardo Luiz Harry Diniz Lemos. Rodrigo de Lima Amaral. Cesar Monzu Freire & Julio Romano Meneghini. Thermodynamical model of an atmospheric steam engine. *Journal of the Brazilian Society of Mechanical Sciences and Engineering* Vol. 43. 493 (2021). <https://doi.org/10.1007/s40430-021-03209-9>.
7. Knowlen C. Williams J. Mattick A. Deparis H. Hertzberg A. Quasi-isothermal expansion engines for liquid nitrogen automotive propulsion. 1997. SAE paper 972649. <https://www.doi.org/10.4271/972649>
8. Cicconardi S. Jannelli E. Perna A. Spazzafumo G. A steam cycle with an isothermal expansion: the effect of flow variation. *Int J Hydrogen Energy* 1999;24(1):53-57. [https://www.doi.org/10.1016/S0360-3199\(98\)00011-1](https://www.doi.org/10.1016/S0360-3199(98)00011-1).
9. Cicconardi S. Jannelli E. Perna A. Spazzafumo G. Parametric analysis of a steam cycle with a quasi-isothermal expansion. *Int J Hydrogen Energy* 2001;26(3): 275-279. [https://www.doi.org/10.1016/S0360-3199\(00\)00036-7](https://www.doi.org/10.1016/S0360-3199(00)00036-7).
10. Park JK. Ro PI. Lim SD. Mazzoleni AP. Quinlan B. Analysis and optimization of a quasi-isothermal compression and expansion cycle for ocean compressed air energy storage (OCAES). In: *Oceans*. 2012. IEEE; 2012. pp. 1-8 <https://www.doi.org/10.1109/OCEANS.2012.6404964>.
11. Kim Y-M. Shin D-G. Lee S-Y. Favrat D. Isothermal transcritical CO₂ cycles with TES for electricity storage. *Energy* 2013;49: 484-501. <https://www.doi.org/10.1016/j.energy.2012.09.057>
12. Opubo N. Igobo. Philip A. Davies. A high-efficiency solar Rankine engine with isothermal expansion. *Int J Low-Carbon Technol*. 2013; 8(Suppl. 1):i27-33. <https://www.doi.org/10.1093/ijlct/ctt031>.
13. [17] Opubo N. Igobo. Philip A. Davies. Review of low-temperature vapor power cycle engines with quasi-isothermal expansion. *Energy* 70 (2014) 22-34. <https://www.doi.org/10.1016/j.energy.2014.03.123>
14. Ferreiro R. Ferreiro B. Isothermal and Adiabatic Expansion Based Trilateral Cycles. *British Journal of Applied Science & Technology*. 2015; (8) 5: 448-460. <https://www.doi.org/10.9734/BJAST/2015/17350>.
15. Ferreiro R. Ferreiro B. The Behavior of Some Working Fluids Applied on the Trilateral Cycles with Isothermal Controlled Expansion. *British Journal of Applied Science & Technology*. 2015; (9) 5: 694-450-463. <https://www.doi.org/10.9734/BJAST/2015/18624>.
16. Ramon Ferreiro Garcia. Jose Carbia Carril. Closed Processes Based Heat-Work Interactions Doing Useful Work by Adding and Releasing Heat. *International Journal of Emerging Engineering Research and Technology*. Volume 6. Issue 11. 2018. pp 8-23. ISSN 2349-4395 (Print) & ISSN 2349-4409 (Online). Accessed at: <https://www.ijeert.org/papers/v6-i11/2.pdf>; <https://www.ijeert.org/v6-i11>.
17. R. Ferreiro Garcia, Power Plants and Cycles: Advances and Trends, Book Publisher International, London 2020, ISBN-13 (15) 978-93-90431-67- 0; <https://doi.org/10.9734/bpi/mono/978-93-90431-59-5>; <http://bp.bookpi.org/index.php/bpi/catalog/book/332>; <https://www.doi.org/10.9734/bpi/mono/978-93-90431-59-5>. Accessed at: [Combined Cycle Consisting](#)

- of Closed Processes Based Cycle Powered by A Reversible Heat Pump that Exceed Carnot Factor | [Journal of advanced in physics \(rajpub.com\)](https://rajpub.com/index.php/jap/article/view/8034); <https://rajpub.com/index.php/jap/article/view/8034>.
18. Ramon Ferreiro Garcia, Jose Carbia Carril, Manuel Romero Gomez and Javier Romero Gomez. Energy and entropy analysis of closed adiabatic expansion based trilateral cycles. *Energy Conversion and Management* 119 (2016) 49–59. <http://dx.doi.org/10.1016/j.enconman.2016.04.031>.
 19. Ramon Ferreiro Garcia. Reply to: Comment on “Energy and entropy analysis of closed adiabatic expansion based trilateral cycles” by Garcia et al. *Energy Conversion and Management* 119 (2016) 49–59. *Energy Conversion and Management* 123 (2016) 646–648. <http://dx.doi.org/10.1016/j.enconman.2016.06.05>.
 20. Ramon Ferreiro Garcia, Jose Carbia Carril. Combined Cycle Consisting of Closed Processes Based Cycle Powered by A Reversible Heat Pump that Exceed Carnot Factor. *Journal of Advances in Physics*, Volume 15, (2018), Pages: 6078–6100. ISSN: 2347-3487. DOI: [10.24297/jap.v15i0.8034](https://doi.org/10.24297/jap.v15i0.8034).
 21. Ramon Ferreiro Garcia. Study of the disruptive design of a thermal power plant implemented by several power units coupled in cascade. *Energy Technol.* 2023, 2300362 (1–17). Published by Wiley-VCH GmbH. DOI: <https://doi.org/10.1002/ente.202300362>.
 22. Ramón Ferreiro Garcia. Efficient disruptive power plant-based heat engines doing work by means of strictly isothermal closed processes. *Journal of Advances in Physics* Vol 22 (2024), p 30.53, ISSN: 2347-3487. <https://rajpub.com/index.php/jap/article/view/9587>. DOI: <https://doi.org/10.24297/jap.v15i0.9587>.
 23. Ramón Ferreiro Garcia. Design study of a disruptive self-powered power plant prototype. *Journal of Advances in Physics* Vol 22 (2024), p 62.92, ISSN: 2347-3487. <https://rajpub.com/index.php/jap/article/view/9596>. DOI: <https://doi.org/10.24297/jap.v22i.9596>.
 24. E. W. Lemmon, M. L. Huber, M. O. McLinden, NIST Reference Fluid Thermodynamic And Transport Properties – REFPROP Version 8.0, User’s Guide, NIST, Boulder, CO. 2007.